The Affine Heston Model with Correlated Gaussian Interest Rates for Pricing Hybrid Derivatives

Lech A. Grzelak,* Cornelis W. Oosterlee,† Sacha van Weeren‡

Abstract

In this article we define a multi-factor equity-interest rate hybrid model with non-zero correlation between the stock and interest rate. The equity part is modeled by the Heston model [24] and we use a Gaussian multi-factor short-rate process [7; 25]. By construction, the model fits in the framework of affine diffusion processes [11] allowing fast calibration to plain vanilla options. We also provide an efficient Monte Carlo simulation scheme.

Key words: Hybrid stochastic model, Heston-Gaussian multi-factor equity-interest rate model, affine diffusion process, characteristic function, unbiased Monte Carlo simulation.

1 Introduction

Pricing modern contracts involving multiple asset classes requires well-developed pricing models from quantitative analysts. Among them the hybrid models, that include features from different asset classes, are of current interest.

In this article we propose a hybrid model based on two particular asset classes: the equity and the interest rates. Such a model can be used for pricing specific hybrid products or for accurate pricing of long-term equity options. Although multi-dimensional hybrids can relatively easily be defined, real use of the models is only guaranteed if the hybrid model is properly defined for each asset class (i.e. a satisfactory fit to implied volatility structures), and if it is possible to set a non-zero correlation structure among the processes from the different asset classes. Furthermore, highly efficient pricing of fundamental contracts needs to be available for model calibration. In this article we propose a model which satisfies these requirements.

We define a multi-factor hybrid model with correlation between the equity and interest rate asset classes, which, by construction, enables efficient pricing of plain vanilla equity options and goes beyond the models with a normally distributed volatility process. We show that the new model can easily be used for calibration and for the pricing of structured products exposed to equity and interest rate risk. The hybrid model is easily understood and an efficient implementation is given.

In the hybrid model the equity part is driven by the Heston model [24], while for the short-rate process a Gaussian multi-factor model [25] is taken with a non-zero correlation between the asset classes. The model belongs to the affine diffusion framework for which the characteristic function can be determined. This facilitates the use of Fourier-based algorithms [9; 14] for efficient pricing of plain vanilla contracts. Additionally, Monte Carlo simulation can be performed by a straightforward generalization of the scheme developed by Andersen in [3]. By defining the affine hybrid Heston model under the forward measure, we can price several financial derivative products (like American options [15]) as under the basic Heston model.

*Delft University of Technology, Delft Institute of Applied Mathematics, Delft, The Netherlands, and Rabobank International, Utrecht. E-mail address: L.A.Grzelak@tudelft.nl.

†CWI – Centrum Wiskunde & Informatica, Amsterdam, the Netherlands, and Delft University of Technology, Delft Institute of Applied Mathematics. E-mail address: C.W.Oosterlee@cwi.nl.

‡Rabobank International, The Netherlands, Utrecht. E-mail address: Sacha.WeerenVan@rabobank.com.

The interest rates are driven by multi-factor Gaussian rates [26]. This model provides a rich pattern for the term structure movements and recovers a *humped* volatility structure observed in the market. The hybrid model under consideration can be used for hybrid payoffs which have a limited sensitivity to the interest rate smile.

For the model considered also the Greeks for plain vanilla options can be efficiently determined and used for hedging. When hedging hybrid products, exposed to different sources of risks coming from equity or interest rate, it is crucial to choose an appropriate set of hedging instruments. Particularly, correlation risk needs to be taken into account here. As it is difficult to find a *pure* correlation product in the market which can be used for hedging, one may consider, similarly as for hedging of jump processes (as presented in [17]), a mean-variance hedging strategy based on a portfolio of stocks, options and interest rate instruments, like caplets and swaptions.

Additionally, due to the sensitivity of the model to different correlations, it is also possible to adjust the risk-related margins.

Pricing long-maturity options with equity-interest rate hybrid models is common practice in the market. In [22; 38] a stochastic volatility equity hybrid model with a full matrix of correlations (the Schöbel-Zhu-Hull-White model) was presented. Approximations for the Heston-Hull-White hybrid model were then presented in [21]. In the same article the interest rate process of Cox-Ingersoll-Ross [10] (CIR) was analyzed. In [2] the Heston model with CIR interest rates was analyzed with respect to forward starting options.

In practice, especially when dealing with long-maturity options or simple hybrid products, the short-rate models are often used. Approximations for hybrids in which the interest rates are driven by the stochastic volatility Libor Market Model have been presented in [23].

This article is divided in several parts. In Section 2 we define the Heston-Gaussian two-factor hybrid model and highlight the affinity problems. In the follow-up section, which is the core of our article, we propose an affine version of this hybrid model. We derive the model under the T-forward measure and provide the corresponding characteristic function. In the same section we describe the derivation of the Greeks as well as Monte Carlo simulation; we also investigate properties like a positive definite correlation matrix. Section 4 is dedicated to the numerical experiments where we compare the affine model to the non-affine Heston hybrid model and the Schöbel-Zhu-Hull-White model, and check the performance for pricing a hybrid product. Section 5 concludes.

2 Hybrid with Multi-Factor Short Rate Process

2.1 Model under the Spot Measure

Suppose we have given two asset classes defined by the vectors $\mathbf{X}^{\bar{n}\times 1}(t)$, $\bar{n} \in \mathbb{N}^+$ for the equity and for the interest rates $\mathbf{R}^{\bar{m}\times 1}(t)$, $\bar{m} \in \mathbb{N}^+$. One can take high-dimensional processes with stochastic volatility, and define the following system of governing stochastic differential equations (SDEs):

$$\begin{cases} \mathrm{d}\mathbf{R}(t) = & a(\mathbf{R}(t))\mathrm{d}t + & b(\mathbf{R}(t))\mathrm{d}\mathbf{W}_{\mathbf{R}}(t), \\ \mathrm{d}\mathbf{X}(t) = & c(\mathbf{X}(t),\mathbf{R}(t))\mathrm{d}t + & d(\mathbf{X}(t))\mathrm{d}\mathbf{W}_{\mathbf{X}}(t), \\ \mathbf{Z}(t)\mathbf{Z}^{\mathrm{t}}(t) = & \mathbf{C}_{\mathbf{H}}\mathrm{d}t, & \end{cases} \tag{2.1}$$

where $\mathbf{H}(t) = [\mathbf{R}(t), \mathbf{X}(t)]^{\mathrm{t}}$, $\mathbf{Z}(t) = [\mathrm{d}\mathbf{W}_{\mathbf{R}}(t), \mathrm{d}\mathbf{W}_{\mathbf{X}}(t)]^{\mathrm{t}}$, $\mathbf{C}_{\mathbf{H}}$ is a $(\bar{n}+\bar{m}) \times (\bar{n}+\bar{m})$ matrix which represents the instantaneous correlation between the Brownian motions [1]. The noises $\mathrm{d}\mathbf{W}_{\cdot}(t)$ are assumed to be multi-dimensional, and correlation within the asset classes is allowed, as well as correlations between these classes.

Since the Heston model in [24] is sufficiently complex for explaining the smile-shaped implied volatilities in equity, we take this model for the equity part. In particular, the

[1] We use superscript "t" for transpose, and superscript "T" to indicate the T-forward measure.

model for the state vector $\mathbf{X}(t) = [v(t), \hat{x}(t) = \log S(t)]^{\mathrm{t}}$ is described by the following system of SDEs:

$$\begin{cases} \mathrm{d}\hat{x}(t) = & (r(t) - 1/2v(t))\,\mathrm{d}t + & \sqrt{v(t)}\mathrm{d}W_x(t), & S(0) > 0, \\ \mathrm{d}v(t) = & \epsilon\,(\bar{v} - v(t))\,\mathrm{d}t + & \omega\sqrt{v(t)}\mathrm{d}W_v(t), & v(0) > 0, \end{cases} \tag{2.2}$$

with $\mathrm{d}W_x(t)\mathrm{d}W_v(t) = \rho_{x,v}\mathrm{d}t$, the speed of mean reversion $\epsilon > 0$; $\bar{v} > 0$ is the long-term mean of the stochastic variance process $v(t)$, and $\omega > 0$ specifies the volatility of the variance process. Note that the term $1/2v(t)$ in the $\hat{x}(t)$-process results from Itô's Lemma when deriving the dynamics for $\log S(t)$.

For the interest rate process we consider the Gaussian multi-factor short-rate model (Gn++) [7], also known as a multi-factor Hull-White model. The model, for a given state vector $\mathbf{R}(t) = [r(t), \zeta_1(t), \ldots, \zeta_{n-1}(t)]^{\mathrm{t}}$, is defined by the following system of SDEs:

$$\begin{cases} \mathrm{d}r(t) = & (\theta(t) + \sum_{k=1}^{n-1} \zeta_k(t) - \kappa r(t))\mathrm{d}t + & \eta\mathrm{d}W_r(t), & r(0) > 0, \\ \mathrm{d}\zeta_k(t) = & -\lambda_k\zeta_k(t)\mathrm{d}t + & \gamma_k\mathrm{d}W_{\zeta_k}(t), & \zeta_k(0) = 0, \end{cases} \tag{2.3}$$

where

$$\mathrm{d}W_r(t)\mathrm{d}W_{\zeta_k}(t) = \rho_{r,\zeta_k}\mathrm{d}t,\ k = 1, \ldots, n-1, \quad \mathrm{d}W_{\zeta_i}(t)\mathrm{d}W_{\zeta_j}(t) = \rho_{\zeta_i,\zeta_j}\mathrm{d}t,\ \ i \neq j,$$

with $\kappa > 0$, $\lambda_k > 0$ the mean reversion parameters; $\eta > 0$ and parameters γ_k determine the volatility magnitude of the interest rate. In the system above, coefficient $\theta(t) > 0$, $t \in \mathbb{R}^+$, stands for long-term interest rate (which is usually calibrated to the current yield curve).

The Gn++ model provides a satisfactory fit to at-the-money humped volatility structure for forward Libor rates. Moreover, the easy construction of the model (based on a multivariate normal distribution) provides closed-form solutions for caps and swaptions, enabling fast calibration. On the other hand, since the model is assumed to be normal, the interest rates can become negative. This however is known and is taken care of in practical applications (see for example [36]).

By taking the equity model $\mathbf{X}(t)$ as introduced in (2.2) and the interest rate part $\mathbf{R}(t)$ from (2.3), a hybrid model $\mathbf{H}(t) = [\mathbf{R}(t), \mathbf{X}(t)]^{\mathrm{t}} = [r(t), \zeta_1(t), \ldots, \zeta_{n-1}(t), v(t), \hat{x}(t)]^{\mathrm{t}}$ can be defined with the following instantaneous correlation structure:

$$\mathbf{C_H} := \left[\begin{array}{cccc|cc} 1 & \rho_{r,\zeta_1} & \cdots & \rho_{r,\zeta_{n-1}} & 0 & \rho_{x,r} \\ \rho_{r,\zeta_1} & 1 & \cdots & \rho_{\zeta_1,\zeta_{n-1}} & 0 & \rho_{x,\zeta_1} \\ \vdots & \vdots & \ddots & \vdots & \vdots & \vdots \\ \rho_{r,\zeta_{n-1}} & \rho_{\zeta_{n-1},\zeta_1} & \cdots & 1 & 0 & \rho_{x,\zeta_{n-1}} \\ \hline 0 & 0 & \cdots & 0 & 1 & \rho_{x,v} \\ \rho_{x,r} & \rho_{x,\zeta_1} & \cdots & \rho_{x,\zeta_{n-1}} & \rho_{x,v} & 1 \end{array}\right]. \tag{2.4}$$

Model $\mathbf{H}(t)$ is the *Heston-Gaussian n-factor hybrid model* (H-Gn++). Note that the equity and the interest rate asset classes are linked by correlations in the right-upper and left-lower diagonal blocks of matrix $\mathbf{C_H}$. Our main objective is the preservation of the correlation, $\rho_{x,r}$, between the log-equity and the interest rate.

As it is nontrivial to hedge equity-interest rate hybrids by liquidly traded standard instruments (see [6] for details), and as the correlations between different asset classes cannot be easily implied from the market, historical estimates are often used. However, as soon as hybrid product prices become available, one can use the additional correlations (degrees of freedom) to enhance the hybrid model performance.

Assuming $V := V(t, \mathbf{H}(t))$ to represent the value of a European claim, we can derive the corresponding pricing partial differential equation (PDE) [18] with the help of the arbitrage-free pricing theorem and the use of Itô's Formula:

$$0 = (r - 1/2v)\frac{\partial V}{\partial \hat{x}} + \epsilon(\bar{v} - v)\frac{\partial V}{\partial v} + \left(\theta(t) + \sum_{k=1}^{n-1}\zeta_k - \kappa r\right)\frac{\partial V}{\partial r} - \sum_{k=1}^{n-1}\lambda_k\zeta_k\frac{\partial V}{\partial \zeta_k} - rV$$
$$+\frac{1}{2}v\frac{\partial^2 V}{\partial \hat{x}^2} + \frac{1}{2}\omega^2 v\frac{\partial^2 V}{\partial v^2} + \frac{1}{2}\eta^2\frac{\partial^2 V}{\partial r^2} + \frac{1}{2}\sum_{k=1}^{n-1}\gamma_k^2\frac{\partial^2 V}{\partial \zeta_k} + \rho_{x,v}\omega v\frac{\partial^2 V}{\partial \hat{x}\partial v} + \rho_{x,r}\eta\sqrt{v}\frac{\partial^2 V}{\partial \hat{x}\partial r}$$
$$+\sqrt{v}\sum_{k=1}^{n-1}\rho_{x,\zeta_k}\gamma_k\frac{\partial^2 V}{\partial \hat{x}\partial \zeta_k} + \sum_{k-1}^{n-1}\rho_{r,\zeta_k}\gamma_k\eta\frac{\partial^2 V}{\partial r\partial \zeta_k} + \frac{\partial V}{\partial t} + \sum_{k=1}^{n-2}\sum_{j=k+1}^{n-1}\rho_{\zeta_k,\zeta_j}\gamma_k\gamma_j\frac{\partial^2 V}{\partial \zeta_k\partial \zeta_j}, \quad (2.5)$$

with specific boundary and final conditions (for details on boundary conditions for similar problems, see, for example, [12] pp.241).

2.1.1 Covariance Structure

The solution of the (n+2)D convection-diffusion-reaction PDE in (2.5) can be approximated by means of standard numerical techniques, like finite differences (see for example [32]). This may however cost substantial CPU time for the model evaluation. An alternative is to use the Feynman-Kac theorem and reformulate the problem as an integral equation related to the discounted expected payoff.

Let us take the following state vector $\mathbf{H} = [r(t), \zeta_1(t), \ldots, \zeta_{n-1}(t), v(t), \hat{x}(t)]^{\mathrm{t}}$, and determine the associated (symmetric) instantaneous covariance matrix $\Sigma_{\mathbf{H}}$ of hybrid model (2.1) with (2.2) and (2.3):

$$\Sigma_{\mathbf{H}} := \left[\begin{array}{cccc|cc} \eta^2 & \rho_{r,\zeta_1}\eta\gamma_1 & \cdots & \rho_{r,\zeta_{n-1}}\eta\gamma_{n-1} & 0 & \rho_{x,r}\eta\sqrt{v} \\ \rho_{r,\zeta_1}\eta\gamma_1 & \gamma_1^2 & \cdots & \rho_{\zeta_1,\zeta_{n-1}}\gamma_1\gamma_{n-1} & 0 & \rho_{x,\zeta_1}\gamma_1\sqrt{v} \\ \vdots & \vdots & \ddots & \vdots & \vdots & \vdots \\ \rho_{r,\zeta_{n-1}}\eta\gamma_{n-1} & \rho_{\zeta_{n-1},\zeta_1}\gamma_{n-1}\gamma_1 & \cdots & \gamma_{n-1}^2 & 0 & \rho_{x,\zeta_{n-1}}\gamma_{n-1}\sqrt{v} \\ \hline 0 & 0 & \cdots & 0 & \omega^2 v & \rho_{x,v}\omega v \\ \rho_{x,r}\eta\sqrt{v} & \rho_{x,\zeta_1}\gamma_1\sqrt{v} & \cdots & \rho_{x,\zeta_{n-1}}\gamma_{n-1}\sqrt{v} & \rho_{x,v}\omega v & v \end{array}\right]. \quad (2.6)$$

For the H-Gn++ hybrid model the instantaneous covariance matrix in (2.6) is not affine ([11]) in all terms of the right-upper block. One can immediately see that the affinity problem disappears for $\rho_{x,r} = 0$ and $\rho_{x,\zeta_k} = 0$, for $k = 1, \ldots, n-1$. This, however, means independence between the asset classes. In order to stay in the affine class with nonzero correlations between the assets, approximations need to be introduced. This is the approach we take here.

In order to define an alternative model which is affine, it appears necessary to relate the instantaneous covariance matrix in (2.6) to the corresponding stochastic differential equations. This can be done by expressing the model in terms of the *independent* Brownian motions, $\widetilde{\mathbf{W}}(t) = [\widetilde{W}_r(t), \widetilde{W}_{\zeta_1}(t), \ldots, \widetilde{W}_{\zeta_{n-1}}(t), \widetilde{W}_v(t), \widetilde{W}_x(t)]^{\mathrm{t}}$. For a state vector $\mathbf{H}(t) = [r(t), \zeta_1(t), \ldots, \zeta_{n-1}(t), v(t), \hat{x}(t)]^{\mathrm{t}}$, the model, in terms of independent Brownian motions, can be rewritten as:

$$\mathrm{d}\mathbf{H}(t) = \mu(\mathbf{H}(t))\mathrm{d}t + \mathbf{A}(t)\mathbf{U}\mathrm{d}\widetilde{\mathbf{W}}(t), \quad (2.7)$$

where $\mu(\mathbf{H}(t))$ represents the drift and $\mathbf{U}$ is the Cholesky lower triangular matrix so that $\mathbf{C}_{\mathbf{H}} = \mathbf{U}\mathbf{U}^{\mathrm{t}}$ for matrix $\mathbf{C}_{\mathbf{H}}$ in (2.4) and matrix $\mathbf{A}(t)$ is given by:

$$\mathbf{A}(t) = \left[\begin{array}{cccc|cc} \eta & 0 & \ldots & 0 & 0 & 0 \\ 0 & \gamma_1 & \ldots & 0 & 0 & 0 \\ \vdots & \vdots & \ddots & \vdots & \vdots & \vdots \\ 0 & 0 & \ldots & \gamma_{n-1} & 0 & 0 \\ \hline 0 & 0 & \ldots & 0 & \omega\sqrt{v(t)} & 0 \\ 0 & 0 & \ldots & 0 & 0 & \sqrt{v(t)} \end{array}\right]. \quad (2.8)$$

Equivalently, Model (2.7) can be expressed as:

$$\mathrm{d}\mathbf{H}(t) = \mu(\mathbf{H}(t))\mathrm{d}t + \mathbf{L}(t)\mathrm{d}\widetilde{\mathbf{W}}(t), \quad (2.9)$$

with

$$\mathbf{L}(t)\mathbf{L}(t)^{\mathrm{t}} = \Sigma_{\mathbf{H}}, \tag{2.10}$$

and $\Sigma_{\mathbf{H}}$ the instantaneous covariance matrix in (2.6).

The model representation of (2.9) is favorable compared to (2.7) since we have a direct relation between the covariance matrix (2.6) and the SDEs.

2.2 Zero-coupon bonds under multi-factor Gaussian model

In the sections to follow we reduce the dimension of the pricing problem by an appropriate measure change, and define an affine version of the multi-factor hybrid model.

In order to derive the multi-factor hybrid model under the *forward measure* the corresponding zero-coupon bond needs to be determined first.

Under the risk-neutral measure, $\mathbb{Q}$, we consider the following n-factor interest rate model:

$$\begin{cases} \mathrm{d}r(t) = & (\theta(t) + \sum_{k=1}^{n-1} \zeta_k(t) - \kappa r(t))\mathrm{d}t + & \eta \mathrm{d}W_r(t), \quad r(0) > 0, \\ \mathrm{d}\zeta_k(t) = & & -\lambda_k \zeta_k(t)\mathrm{d}t + \quad \gamma_k \mathrm{d}W_{\zeta_k}(t), \quad \zeta_k(0) = 0, \end{cases} \tag{2.11}$$

with a full correlation matrix with $\rho_{r,\zeta_i} \neq 0$, and $\rho_{\zeta_i,\zeta_j} \neq 0$ for $i, j = \{1, \ldots, n-1\}$, $i \neq j$.

This model is affine in all state variables, so we can derive the corresponding characteristic function (see [11]) for $r(T)$:

$$\begin{aligned} \phi_{\mathrm{Gn++}}(u, r(t), \tau) &= \mathbb{E}^{\mathbb{Q}}\left(\mathrm{e}^{-\int_t^T r(s)\mathrm{d}s} \mathrm{e}^{iur(T)} \middle| \mathcal{F}(t)\right) \\ &= \exp\left(A(u,\tau) + B(u,\tau)r(t) + \sum_{k=1}^{n-1} C_k(u,\tau)\zeta_k(t)\right), \end{aligned} \tag{2.12}$$

with final condition $\phi_{\mathrm{Gn++}}(u, r(T), 0) = \mathrm{e}^{iur(T)}$, where conventionally $\tau = T - t$. The functions $A(u,\tau)$, $B(u,\tau)$ and $C_k(u,\tau)$ are known explicitly and are given by the set of Riccati-type ODEs:

$$\begin{aligned} B'(u,\tau) &= -1 - \kappa B(u,\tau), \\ C_k'(u,\tau) &= B(u,\tau) - \lambda_k C_k(u,\tau), \\ A'(u,\tau) &= \theta(t)B(u,\tau) + \frac{1}{2}\eta^2 B^2(u,\tau) + \eta \sum_{k=1}^{n-1} \rho_{r,\zeta_k}\gamma_k B(u,\tau)C(u,\tau) \\ &\quad + \frac{1}{2}\sum_{i=1}^{n-1}\sum_{j=1}^{n-1} \rho_{\zeta_i,\zeta_j}\gamma_i\gamma_j C_i(u,\tau)C_j(u,\tau), \end{aligned} \tag{2.13}$$

with boundary conditions $B(u,0) = iu$, $C_k(u,0) = 0$ and $A(u,0) = 0$. These ODEs can be solved analytically. By setting $u = 0$ in (2.12) the zero-coupon bond price is obtained, i.e.:

$$P(t,T) \triangleq \mathbb{E}^{\mathbb{Q}}\left(\mathrm{e}^{-\int_t^T r(s)\mathrm{d}s} \middle| \mathcal{F}(t)\right) = \exp\left(A(t,T) + B(t,T)r(t) + \sum_{k=1}^{n-1} C_k(t,T)\zeta_k(t)\right), \tag{2.14}$$

where

$$A(t,T) := A(0,\tau), \quad B(t,T) := B(0,\tau), \quad C_k(t,T) := C_k(0,\tau). \tag{2.15}$$

By applying Itô's Lemma to Equation (2.14), the zero-coupon bond dynamics under the $\mathbb{Q}$ measure read:

$$\frac{\mathrm{d}P(t,T)}{P(t,T)} = r(t)\mathrm{d}t + \eta B(t,T)\mathrm{d}W_r(t) + \sum_{k=1}^{n-1} \gamma_k C_k(t,T)\mathrm{d}W_{\zeta_k}(t), \tag{2.16}$$

where the functions $B(t,T)$ and $C_k(t,T)$ satisfy the ODEs (2.13) via (2.15). Their solution reads:

$$B(t,T) = \frac{1}{\kappa}\left(\mathrm{e}^{-\kappa(T-t)}-1\right), \tag{2.17}$$

$$C_k(t,T) = \frac{1}{\kappa(\lambda_k-\kappa)}\mathrm{e}^{-\kappa(T-t)} - \frac{1}{\lambda_k(\lambda_k-\kappa)}\mathrm{e}^{-\lambda_k(T-t)} - \frac{1}{\lambda_k\kappa}, \tag{2.18}$$

with

$$C_k(t,T) = \frac{1}{\kappa^2}\left(\mathrm{e}^{-\kappa(T-t)}(1+\kappa(T-t))-1\right), \quad \text{for } \lambda_k \to \kappa,$$

and $k = \{1,\ldots,n-1\}$.

The dynamics for the zero-coupon bond are important when switching measures in the hybrid model.

3 The Affine Heston-Gn++ Model (AH-Gn++)

In this section, which is the main part of the article, we define *the affine hybrid Heston model*. Since the model proposed is, by its structure, similar to the Heston-multi-factor-Gaussian model (denoted by H-Gn++) we abbreviated the model by "AH-Gn++", which stands for "affine version of the H-Gn++ model".

For convenience, we start with $n = 2$. The AH-G2++ model with the state vector $\mathbf{H}(t) = [r(t), \zeta(t), v(t), S(t)]^{\mathrm{t}}$ under the risk-neutral measure $\mathbb{Q}$, is given by the following system of SDEs:

$$\begin{bmatrix} \mathrm{d}r(t) \\ \mathrm{d}\zeta(t) \\ \mathrm{d}v(t) \\ \mathrm{d}S(t)/S(t) \end{bmatrix} = \begin{bmatrix} \theta(t)+\zeta(t)-\kappa r(t), \\ -\lambda\zeta(t) \\ \epsilon(\bar{v}-v(t)) \\ r(t) \end{bmatrix} \mathrm{d}t + \mathbf{L}(t) \begin{bmatrix} \mathrm{d}\widetilde{W}_r(t) \\ \mathrm{d}\widetilde{W}_\zeta(t) \\ \mathrm{d}\widetilde{W}_v(t) \\ \mathrm{d}\widetilde{W}_x(t) \end{bmatrix}, \tag{3.1}$$

where

$$\mathbf{L}(t)\mathbf{L}(t)^{\mathrm{t}} = \left[\begin{array}{cc|cc} \eta^2 & \rho_{r,\zeta}\eta\gamma & 0 & \rho_{x,r}\eta\alpha(t) \\ \rho_{r,\zeta}\gamma\eta & \gamma^2 & 0 & \rho_{x,\zeta}\gamma\alpha(t) \\ \hline 0 & 0 & \omega^2 v & \rho_{x,v}\omega v \\ \rho_{x,r}\eta\alpha(t) & \rho_{x,\zeta}\gamma\alpha(t) & \rho_{x,v}\omega v & v \end{array}\right] =: \Sigma_{\mathbf{H}}. \tag{3.2}$$

Here, the function $\alpha(t)$ is a deterministic function depending on time t, which will be discussed in Section 3.3. With deterministic function $\alpha(t)$, matrix $\Sigma_{\mathbf{H}}$ in (3.2) does not contain any non-affine elements, so that the AH-G2++ model belongs to the class of affine processes. This allows us to determine the characteristic function for the model.

Application of the Cholesky decomposition to matrix $\Sigma_{\mathbf{H}}$ in (3.2) gives for matrix $\mathbf{L}(t)$:

$$\mathbf{L}(t) = \begin{bmatrix} \eta & 0 & 0 & 0 \\ \gamma\mathbf{U}_{2,1} & \gamma\mathbf{U}_{2,2} & 0 & 0 \\ 0 & 0 & \omega\sqrt{v(t)} & 0 \\ \alpha(t)\mathbf{U}_{4,1} & \alpha(t)\mathbf{U}_{4,2} & \mathbf{U}_{4,3}\sqrt{v(t)} & \sqrt{v(t)(1-\mathbf{U}_{4,3}^2)-\alpha^2(t)\left(\mathbf{U}_{4,1}^2+\mathbf{U}_{4,2}^2\right)} \end{bmatrix}, \tag{3.3}$$

where $\mathbf{U}$ is the lower triangular Cholesky matrix obtained from the correlation matrix, with values for $\mathbf{U}_{i,j}$ given by:

$$\begin{cases} \mathbf{U}_{2,1} = \rho_{r,\zeta}, \quad \mathbf{U}_{4,1} = \rho_{x,r}, \quad \mathbf{U}_{4,3} = \rho_{x,v}, \\ \mathbf{U}_{2,2} = \sqrt{1-\rho_{r,\zeta}^2}, \quad \mathbf{U}_{4,2} = \left(\rho_{x,\zeta}-\rho_{x,r}\rho_{r,\zeta}\right)/\sqrt{1-\rho_{r,\zeta}^2}. \end{cases} \tag{3.4}$$

The correlation structure between equity and interest rate in the AH-G2++ model in (3.1) with (3.2) is dependent on function $\alpha(t)$. If we set, for example, $\alpha(t) \equiv 0$, independence between the asset classes is imposed. Our main objective is to choose a function $\alpha(t)$ so that the AH-G2++ model stays affine and that it resembles the full-scale H-G2++ model. In Section 3.3 we discuss a particular choice for $\alpha(t)$.

3.1 The Affine Hybrid Model Under Measure Change

It is common to move the model from the spot measure, generated by the money-savings account, $M(t)$, to the *forward measure* where the numéraire is the zero-coupon bond, $P(t,T)$. As indicated in [34], the forward is defined as,

$$F(t) = \frac{S(t)}{P(t,T)} = \frac{\mathrm{e}^{\hat{x}(t)}}{P(t,T)}, \tag{3.5}$$

where $F(t)$ represents the forward, $S(t)$ stands for stock, $\hat{x}(t)$ is log-stock defined in (2.2) and $P(t,T)$ as defined in (2.16) represents the value of the zero-coupon bond paying €1 at maturity T.

Under the AH-G2++ hybrid model the stock dynamics in terms of independent Brownian motions, are given by:

$$\begin{aligned}\frac{\mathrm{d}S(t)}{S(t)} &= r(t)\mathrm{d}t + \psi_1(t)\mathrm{d}\widetilde{W}_r(t) + \psi_2(t)\mathrm{d}\widetilde{W}_\zeta(t) + \psi_3(t)\sqrt{v(t)}\mathrm{d}\widetilde{W}_v(t) \\ &\quad + \sqrt{v(t)\psi_4(t) + \psi_5(t)}\mathrm{d}\widetilde{W}_x(t),\end{aligned} \tag{3.6}$$

with $\psi_1(t) = \mathbf{U}_{4,1}\alpha(t)$, $\psi_2(t) = \mathbf{U}_{4,2}\alpha(t)$, $\psi_3(t) = \mathbf{U}_{4,3}$, $\psi_4(t) = 1 - \mathbf{U}_{4,3}^2$ and $\psi_5(t) = -\alpha^2(t)\left(\mathbf{U}_{4,1}^2 + \mathbf{U}_{4,2}^2\right)$ where $\mathbf{U}_{i,j}$ is defined by (3.4) and the time-dependent function $\alpha(t)$.

The zero-coupon bond, $P(t,T)$, in terms of independent Brownian motions is defined as:

$$\begin{aligned}\frac{\mathrm{d}P(t,T)}{P(t,T)} &= r(t)\mathrm{d}t + \left(\eta B(t,T) + \rho_{r,\zeta}\gamma C(t,T)\right)\mathrm{d}\widetilde{W}_r(t) \\ &\quad + \gamma C(t,T)\sqrt{1-\rho_{r,\zeta}^2}\mathrm{d}\widetilde{W}_\zeta(t),\end{aligned} \tag{3.7}$$

with $B(t,T)$ in (2.17) and $C(t,T)$ in (2.18). By switching from the risk-neutral measure, $\mathbb{Q}$, to the T-forward measure, $\mathbb{Q}^T$, the discounting will be *decoupled* from taking the expectation, i.e.:

$$\Pi(t) = P(t,T)\mathbb{E}^T\left(\max\left(F(T) - K, 0\right)|\mathcal{F}(t)\right). \tag{3.8}$$

In order to determine the dynamics for $F(t)$ in (3.5), we apply Itô's Formula:

$$\begin{aligned}\frac{\mathrm{d}F(t)}{F(t)} &= \left(\gamma^2C^2 + B\eta(B\eta - \psi_1(t)) + \gamma C\left(2\rho_{r,\zeta}\eta B - \rho_{r,\zeta}\psi_1(t) - \sqrt{1-\rho_{r,\zeta}^2}\psi_2(t)\right)\right)\mathrm{d}t \\ &\quad + \hat{\psi}_1(t)\mathrm{d}\widetilde{W}_r(t) + \hat{\psi}_2(t)\mathrm{d}\widetilde{W}_\zeta(t) + \psi_3(t)\sqrt{v(t)}\mathrm{d}\widetilde{W}_v(t) + \sqrt{v(t)\psi_4(t) + \psi_5(t)}\mathrm{d}\widetilde{W}_x(t),\end{aligned} \tag{3.9}$$

with $\hat{\psi}_1(t) := \psi_1(t) - (\rho_{r,\zeta}\gamma C + \eta B)$, $\hat{\psi}_2(t) := \psi_2(t) - \gamma C\sqrt{1-\rho_{r,\zeta}^2}$ and, for the sake of notation, we have set $B := B(t,T)$ and $C := C(t,T)$.

Forward $F(t)$ is a martingale under the T-forward measure, i.e.,

$$P(t,T)\mathbb{E}^T(F(T)|\mathcal{F}(t)) = P(t,T)F(t),$$

and the corresponding Brownian motions under the T-forward measure, $\mathrm{d}\widetilde{W}_x^T(t)$, $\mathrm{d}\widetilde{W}_v^T(t)$, $\mathrm{d}\widetilde{W}_r^T(t)$ and $\mathrm{d}\widetilde{W}_\zeta^T(t)$, need to be determined.

A change of measure from the spot to the T-forward measure requires a change of numéraire from the money-savings account, $M(t)$, to the zero-coupon bond, $P(t,T)$. In the model we assumed non-zero correlations between interest rates and equity, and all the processes within each asset class, which implies that all processes, except the variance, will change their dynamics by changing the measure.

The lemma below provides the model dynamics under the T-forward measure, $\mathbb{Q}^T$.

Lemma 3.1 (The AH-G2++ model dynamics under the $\mathbb{Q}^T$ measure)**.** *Under the T-forward measure, the AH-G2++ model is governed by the following dynamics:*

$$\begin{aligned}\frac{\mathrm{d}F(t)}{F(t)} &= \hat{\psi}_1(t)\mathrm{d}\widetilde{W}_r^T(t) + \hat{\psi}_2(t)\mathrm{d}\widetilde{W}_\zeta^T(t) + \psi_3(t)\sqrt{v(t)}\mathrm{d}\widetilde{W}_v^T(t) \quad (3.10)\\ &\quad + \sqrt{v(t)\psi_4(t)+\psi_5(t)}\mathrm{d}\widetilde{W}_x^T(t), \quad (3.11)\\ \mathrm{d}v(t) &= \epsilon(\bar{v}-v(t))\mathrm{d}t + \omega\sqrt{v(t)}\mathrm{d}\widetilde{W}_v^T(t),\end{aligned}$$

where $\hat{\psi}_1(t)$ and $\hat{\psi}_2(t)$ are defined as in (3.9) and $\psi_i(t)$, $i=\{1,\ldots,5\}$ as in (3.6) with

$$\begin{aligned}\mathrm{d}r(t) &= \left(\hat{\theta}(t)+\zeta(t)-\kappa r(t)\right)\mathrm{d}t + \eta\mathrm{d}\widetilde{W}_r^T(t),\\ \mathrm{d}\zeta(t) &= \left(-\lambda\zeta(t)+\gamma\eta\rho_{r,\zeta}B(t,T)+\gamma^2C(t,T)\right)\mathrm{d}t + \gamma\rho_{r,\zeta}\mathrm{d}\widetilde{W}_r^T(t) + \gamma\sqrt{1-\rho_{r,\zeta}^2}\mathrm{d}\widetilde{W}_\zeta^T(t),\end{aligned}$$

with $\hat{\theta}(t)=\theta(t)+\eta^2B(t,T)+\rho_{r,\zeta}\eta\gamma C(t,T)$, with a correlation matrix given in (2.4), and with $B(t,T)$, $C(t,T)$ in (2.17) and (2.18).

Since the interest rates are Gaussian, and in the corresponding SDEs the diffusion parts are independent of the state variables, the dimension of the underlying pricing problem is reduced under the T-forward measure (as the forward, $F(t)$, and the variance process, $v(t)$, do not contain $r(t)$ or $\zeta(t)$).

Proof. We express the model in terms of the independent Brownian motions as:

$$\mathrm{d}\mathbf{H}(t) = \mu(\mathbf{H}(t))\mathrm{d}t + \mathbf{L}(t)\mathrm{d}\widetilde{\mathbf{W}}(t), \quad (3.12)$$

where $\mu(\mathbf{H}(t))$ represents the drift and $\mathbf{L}(t)$ is defined in (3.3). Now, we determine the Radon-Nikodým derivative [19], $\Lambda_{\mathbb{Q}}^T(t)$,:

$$\Lambda_{\mathbb{Q}}^T(t) = \frac{\mathrm{d}\mathbb{Q}^T}{\mathrm{d}\mathbb{Q}}\Big|_{\mathcal{F}(t)} = \frac{P(t,T)}{P(0,T)M(t)}, \quad (3.13)$$

where $P(t,T)$ is a zero-coupon bond and $M(t)$ is the money-savings account. By calculating the Itô Derivative of Equation (3.13) we get:

$$\begin{aligned}\frac{\mathrm{d}\Lambda_{\mathbb{Q}}^T}{\Lambda_{\mathbb{Q}}^T} &= \eta B(t,T)\mathrm{d}\widetilde{W}_r(t) + \gamma C(t,T)\left(\rho_{r,\zeta}\mathrm{d}\widetilde{W}_r(t) + \sqrt{1-\rho_{r,\zeta}^2}\mathrm{d}\widetilde{W}_\zeta(t)\right)\\ &= \left(\eta B(t,T)+\rho_{r,\zeta}\gamma C(t,T)\right)\mathrm{d}\widetilde{W}_r(t) + \gamma C(t,T)\sqrt{1-\rho_{r,\zeta}^2}\mathrm{d}\widetilde{W}_\zeta(t). \quad (3.14)\end{aligned}$$

The representation above shows the *Girsanov kernel* which describes the transition from $\mathbb{Q}$ to $\mathbb{Q}^T$, i.e.,

$$\mathrm{d}\widetilde{\mathbf{W}}^T(t) = \Xi(t)\mathrm{d}t + \mathrm{d}\widetilde{\mathbf{W}}(t).$$

So,

$$\mathrm{d}\widetilde{\mathbf{W}}(t) := \begin{bmatrix}\mathrm{d}\widetilde{W}_r(t)\\ \mathrm{d}\widetilde{W}_\zeta(t)\\ \mathrm{d}\widetilde{W}_v(t)\\ \mathrm{d}\widetilde{W}_x(t)\end{bmatrix} = \begin{bmatrix}\mathrm{d}\widetilde{W}_r^T(t)\\ \mathrm{d}\widetilde{W}_\zeta^T(t)\\ \mathrm{d}\widetilde{W}_v^T(t)\\ \mathrm{d}\widetilde{W}_x^T(t)\end{bmatrix} + \begin{bmatrix}\eta B(t,T)+\rho_{r,\zeta}\gamma C(t,T)\\ \gamma C(t,T)\sqrt{1-\rho_{r,\zeta}^2}\\ 0\\ 0\end{bmatrix}\mathrm{d}t. \quad (3.15)$$

Now, by substitution of $\mathrm{d}\widetilde{\mathbf{W}}(t)$ from (3.15) in (3.12) and appropriate substitutions the proof is finalized. □

3.2 The Log-transform and the Characteristic Function

Under the log-transform, $x(t) := \log F(t)$, we obtain the following model dynamics:

$$\begin{aligned}\mathrm{d}x(t) &= -\frac{1}{2}\left(\hat{\psi}_1^2(t)+\hat{\psi}_2^2(t)+\psi_5(t)+v(t)\left(\psi_3^2(t)+\psi_4(t)\right)\right)\mathrm{d}t + \hat{\psi}_1(t)\mathrm{d}\widetilde{W}_r^T(t)\\ &\quad + \hat{\psi}_2(t)\mathrm{d}\widetilde{W}_\zeta^T(t) + \psi_3(t)\sqrt{v(t)}\mathrm{d}\widetilde{W}_v^T(t) + \sqrt{v(t)\psi_4(t)+\psi_5(t)}\mathrm{d}\widetilde{W}_x^T(t) \quad (3.16)\\ \mathrm{d}v(t) &= \epsilon(\bar{v}-v(t))\mathrm{d}t + \omega\sqrt{v(t)}\mathrm{d}\widetilde{W}_v^T(t), \quad (3.17)\end{aligned}$$

with independent Brownian motions, $\mathrm{d}\widetilde{W}_r^T(t)$, $\mathrm{d}\widetilde{W}_\zeta^T(t)$, $\mathrm{d}\widetilde{W}_v^T(t)$ and $\mathrm{d}\widetilde{W}_x^T(t)$. The remaining parameters are as in (3.1). With the closed-form expressions for $\hat{\psi}_1(t)$, $\hat{\psi}_2(t)$, $\psi_3(t)$, $\psi_4(t)$ and $\psi_5(t)$:

$$\begin{aligned}
\hat{\psi}_1(t) &= \alpha(t)\mathbf{U}_{4,1} - (\rho_{r,\zeta}\gamma C(t,T) + \eta B(t,T)),\\
\hat{\psi}_2(t) &= \alpha(t)\mathbf{U}_{4,2} - \gamma C(t,T)\sqrt{1-\rho_{r,\zeta}^2},\\
\psi_3(t) &= \mathbf{U}_{4,3},\\
\psi_4(t) &= 1 - \mathbf{U}_{4,3}^2,\\
\psi_5(t) &= -\alpha^2(t)\left(\mathbf{U}_{4,1}^2 + \mathbf{U}_{4,2}^2\right),
\end{aligned}$$

and $\mathbf{U}$ the Cholesky matrix in (3.4), the dynamics in (3.16) can be simplified:

$$\begin{aligned}
\mathrm{d}x(t) &= \frac{1}{2}\left(\chi(t,T) - v(t)\right)\mathrm{d}t + \hat{\psi}_1(t)\mathrm{d}\widetilde{W}_r^T(t) + \hat{\psi}_2(t)\mathrm{d}\widetilde{W}_\zeta^T(t) + \psi_3(t)\sqrt{v(t)}\mathrm{d}\widetilde{W}_v^T(t)\\
&\quad + \sqrt{v(t)\psi_4(t) + \psi_5(t)}\mathrm{d}\widetilde{W}_x^T(t),
\end{aligned} \tag{3.18}$$

with:

$$\begin{aligned}
\chi(t,T) &= -\gamma^2 C^2(t,T) - \eta^2 B^2(t,T) - 2\rho_{r,\zeta}\gamma\eta B(t,T)C(t,T)\\
&\quad + 2\alpha(t)\Big(\rho_{x,r}\eta B(t,T) + \rho_{x,\zeta}\gamma C(t,T)\Big).
\end{aligned} \tag{3.19}$$

For the log-forward, $x(t)$, the Fokker-Planck equation for $V(t) := V(t,\mathbf{H}(t))$ with $\mathbf{H}(t) = [x(t), v(t)]^{\mathrm{t}}$ is given by:

$$\begin{aligned}
-\frac{\partial V}{\partial t} &= \epsilon(\bar{v} - v)\frac{\partial V}{\partial v} + \frac{1}{2}\left(v - \chi(t,T)\right)\left(\frac{\partial^2 V}{\partial x^2} - \frac{\partial V}{\partial x}\right)\\
&\quad + \frac{1}{2}\omega^2 v\frac{\partial^2 V}{\partial v^2} + \rho_{x,v}\omega v\frac{\partial^2 V}{\partial x \partial v},
\end{aligned} \tag{3.20}$$

with the deterministic, time-dependent function $\chi(t,T)$ in (3.19).

For the affine model, with $\tau = T - t$, the forward characteristic function is of the following form:

$$\phi^T(u, x(t), \tau) = \mathbb{E}^T\left(\mathrm{e}^{iux(T)}|\mathcal{F}(t)\right) = \mathrm{e}^{\hat{A}(u,\tau) + \hat{B}(u,\tau)x(t) + \hat{C}(u,\tau)v(t)}, \tag{3.21}$$

with terminal condition $\phi^T(u, x(T), 0) = \mathrm{e}^{iux(T)}$. Functions $\hat{A}(u,\tau)$, $\hat{B}(u,\tau)$ and $\hat{C}(u,\tau)$ satisfy, using $\hat{\mathbf{B}}(u,\tau) = [\hat{B}(u,\tau), \hat{C}(u,\tau)]^{\mathrm{t}}$, the following Riccati ordinary differential equations (see [11]):

$$\begin{cases}
\dfrac{\mathrm{d}}{\mathrm{d}\tau}\hat{\mathbf{B}}(u,\tau) = & -r_1 + a_1^{\mathrm{T}}\hat{\mathbf{B}}(u,\tau) + & \dfrac{1}{2}\hat{\mathbf{B}}^{\mathrm{T}}(u,\tau)c_1\hat{\mathbf{B}}(u,\tau),\\
\dfrac{\mathrm{d}}{\mathrm{d}\tau}\hat{A}(u,\tau) = & -r_0 + \hat{\mathbf{B}}^{\mathrm{T}}(u,\tau)a_0 + & \dfrac{1}{2}\hat{\mathbf{B}}^{\mathrm{T}}(u,\tau)c_0\hat{\mathbf{B}}(u,\tau).
\end{cases} \tag{3.22}$$

Here, $a_i, c_i, r_i,\ i = 0, 1$, are given by a linear decomposition:

$$\begin{aligned}
\mu_{\mathbf{H}} &= a_0 + a_1\mathbf{H}(t),\ \text{for any } (a_0, a_1) \in \mathbb{R}^l \times \mathbb{R}^{l\times l},\\
\Sigma_{\mathbf{H}}\Sigma_{\mathbf{H}}^{\mathrm{T}} &= (c_0)_{ij} + (c_1)_{ij}^{\mathrm{T}}\mathbf{H}(t),\ \text{for arbitrary } (c_0, c_1) \in \mathbb{R}^{l\times l} \times \mathbb{R}^{l\times l\times l},\\
r_{\mathbf{H}} &= r_0 + r_1^{\mathrm{T}}\mathbf{H}(t),\ \text{for } (r_0, r_1) \in \mathbb{R} \times \mathbb{R}^l,
\end{aligned}$$

where l indicates the dimension of the state vector $\mathbf{H}(t)$. The forward characteristic function in (3.21) is defined by:

$$\begin{aligned}
\hat{B}'(\tau) &= 0,\\
\hat{C}'(\tau) &= 1/2(\hat{B}^2(\tau) - \hat{B}(\tau)) + (\rho_{x,v}\omega\hat{B}(\tau) - \epsilon)\hat{C}(\tau) + 1/2\omega^2\hat{C}^2(\tau),\\
\hat{A}'(\tau) &= \epsilon\bar{v}\hat{C}(\tau) - 1/2\chi(t,T)(\hat{B}^2(\tau) - \hat{B}(\tau)),
\end{aligned}$$

with $\chi(t,T)$ in (3.19), $\hat{B}(0) = iu$, $\hat{C}(0) = 0$ and $\hat{A}(0) = 0$. The ODEs are of *Heston-type* [24], so that the solution is given in closed-form as $\hat{B}(u,\tau) = iu$, and

$$\hat{C}(u,\tau) = \frac{1-\mathrm{e}^{-d_1\tau}}{\omega^2\left(1-g\mathrm{e}^{-d_1\tau}\right)}\left(\epsilon - \rho_{x,v}\omega iu - d_1\right), \tag{3.23}$$

and for $\hat{A}(u,\tau)$ we find:

$$\begin{aligned}\hat{A}(u,\tau) &= \frac{\epsilon\bar{v}}{\omega^2}\left[\left(\epsilon - \rho_{x,v}\omega iu - d_1\right)\tau - 2\log\left(\frac{1-g\mathrm{e}^{-d_1\tau}}{1-g}\right)\right] \\ &\quad + \frac{1}{2}(u^2+iu)\int_0^\tau \chi(T-s,T)\mathrm{d}s,\end{aligned} \tag{3.24}$$

with $d_1 = \sqrt{\left(\rho_{x,v}\omega iu - \epsilon\right)^2 + \omega^2\left(u^2+iu\right)}$, and $g = \frac{-\rho_{x,v}\omega iu + \epsilon - d_1}{-\rho_{x,v}\omega iu + \epsilon + d_1}$, and $\chi(t,T)$ defined in (3.19).

The integral in (3.24) of the deterministic function $\chi(t,T)$ can be calculated explicitly. This integral does not contain the Fourier argument "u" which implies that for pricing a whole strip of strikes, one computation suffices. This is an advantage compared to other hybrid models, like the Schöbel-Zhu-Hull-White model, where each argument, u, requires the calculation of an integral.

Remark (Extension to an n-factor Affine Model)**.** *In Section 3.1 we have shown that switching between the measures, from the spot to the forward, reduces the complexity of the corresponding PDE for the forward price $F(t)$ considerably. By taking Gaussian interest rates the forward dynamics for $F(t)$ do not depend on interest rate variables, as only volatility coefficients from the interest rate processes are present. The generalization from a two-factor interest rate model to an n-factor model does therefore not complicate the pricing problem- it is merely a change of coefficients.*

It is easy to deduce that under the AH-Gn++ model the Fokker-Planck equation for $V(t) := V(t,\mathbf{H}(t))$ with $\mathbf{H}(t) = [x(t),v(t)]^{\mathrm{t}}$ is given by:

$$\begin{aligned}-\frac{\partial V}{\partial t} &= \epsilon(\bar{v}-v)\frac{\partial V}{\partial v} + \frac{1}{2}\left(v - \hat{\chi}(t,T)\right)\left(\frac{\partial^2 V}{\partial x^2} - \frac{\partial V}{\partial x}\right) \\ &\quad + \frac{1}{2}\omega^2 v\frac{\partial^2 V}{\partial v^2} + \rho_{x,v}\omega v\frac{\partial^2 V}{\partial x \partial v},\end{aligned} \tag{3.25}$$

with function $\hat{\chi}(t,T)$ given by:

$$\begin{aligned}\hat{\chi}(t,T) &= -\sum_{i=1}^{n-1}\sum_{j=1}^{n-1}\rho_{\zeta_i,\zeta_j}\gamma_i\gamma_j C_i(t,T)C_j(t,T) - 2\eta B(t,T)\sum_{k=1}^{n-1}\rho_{r,\zeta_k}\gamma_k C_k(t,T) \\ &\quad -\eta^2 B^2(t,T) + 2\alpha(t)\Big(\rho_{x,r}\eta B(t,T) + \sum_{k=1}^{n-1}\rho_{x,\zeta_k}\gamma_k C_k(t,T)\Big),\end{aligned} \tag{3.26}$$

with $B(t,T)$ and $C_k(t,T)$ defined in (2.17) and (2.18), a certain deterministic function $\alpha(t)$ and all the parameters as defined in (2.2) and (2.3).

Since the PDE structure in (3.25) of the AH-Gn++ model is the same as for the AH-G2++ model in (2.5), the results from Section 3.2 can directly be used (only the function $\chi(t,T)$ in (3.24) needs to be replaced by $\hat{\chi}(t,T)$ from (3.26)).

3.2.1 Positive Definiteness of the Covariance Matrix $\Sigma_{\mathbf{H}}$

When performing a simulation of a model, either by a Monte Carlo method or by finite-differences for the associated PDE, the corresponding covariance matrix needs to be defined properly.

Since $\mathbf{L}(t)$ in the AH-G2++ model is obtained from the Cholesky decomposition of the covariance matrix, $\mathbf{L}(t)\mathbf{L}(t)^{\mathrm{t}} = \Sigma_{\mathbf{H}}$, we need to determine under which conditions matrix $\Sigma_{\mathbf{H}}$ is positive definite.

Positive definiteness of the covariance matrix is necessary for performing a Monte Carlo simulation.

Since we deal with a 2×2 covariance matrix (by the change of measure the number of state variables was reduced from four to two), we use Sylvester's Criterion to determine whether the covariance matrix is positive-definite. For a 2×2-matrix the criterion states that a Hermitian matrix is positive definite if the upper left element of matrix $\Sigma_{\mathbf{H}}$ and matrix $\Sigma_{\mathbf{H}}$ itself have positive determinants.

Covariance matrix $\Sigma_{\mathbf{H}}$ is given by:

$$\Sigma_{\mathbf{H}} = \frac{1}{2}\begin{bmatrix} (v(t)-\chi(t,T)) & \rho_{x,v}\omega v(t) \\ \rho_{x,v}\omega v(t) & \omega^2 v(t) \end{bmatrix}, \tag{3.27}$$

with $\chi(t,T)$ in (3.19).

We check when $v(t) > \chi(t,T)$. Since we deal with a non-negative square-root process for $v(t)$, the expression on the left-hand side is always non-negative, i.e., $v(t) \geq 0$. By (3.19) we can rewrite $\chi(t,T)$ as:

$$\begin{aligned} \chi(t,T) &= -\left(\gamma C(t,T) + \rho_{r,\zeta}\eta B(t,T)\right)^2 - \eta^2 B^2(t,T)\left(1-\rho_{r,\zeta}^2\right) \\ &\quad +2\alpha(t)\Big(\rho_{x,r}\eta B(t,T) + \rho_{x,\zeta}\gamma C(t,T)\Big). \end{aligned}$$

Since $B(t,T) \leq 0$ and $C(t,T) \leq 0$ for any $t \leq T$ and $\lambda > 0$, $\kappa > 0$, by setting $\rho_{x,r} > 0$ and $\rho_{x,\zeta} > 0$ the expression for $\chi(t,T)$ is negative guaranteeing that the condition for positive definiteness is satisfied. In the case $\rho_{x,r} < 0$ or $\rho_{x,\zeta} < 0$, the inequality $v(t) > \chi(t,T)$ needs to be satisfied, which is typically is not a problem, especially for large values of $v(t)$.

For the determinant of matrix $\Sigma_{\mathbf{H}}$ we find:

$$\det \Sigma_{\mathbf{H}} = \omega^2 v(t)\left(v(t)-\chi(t,T)\right) - \rho_{x,v}^2\omega^2 v^2(t) \quad > \quad 0, \tag{3.28}$$

which can be expressed as:

$$v(t)(1-\rho_{x,v}^2) \quad > \quad \chi(t,T). \tag{3.29}$$

As before the left-hand side of Inequality (3.29) is positive for $|\rho_{x,v}| < 1$ and $v(t) > 0$ whereas $\chi(t,T)$ is negative for the conditions described before.

3.3 The function $\alpha(t)$

In this section we determine function $\alpha(t)$ in (3.2) for the AH-Gn++ model. In the H-Gn++ model each of the non-affine terms contains the term $\sqrt{v(t)}$, where $v(t)$ is the square-root process defined in (3.1) with dynamics:

$$\mathrm{d}v(t) = \epsilon(\bar{v}-v(t))\mathrm{d}t + \omega\sqrt{v(t)}\mathrm{d}\widetilde{W}_v(t), \tag{3.30}$$

(with all the parameters specified in (2.2)). Since function $\alpha(t)$ is related to the $\sqrt{v(t)}$-term in the H-Gn++ model, a natural definition for $\alpha(t)$ in the AH-Gn++ model appears to be:

$$\alpha(t) := \mathbb{E}(\sqrt{v(t)}), \tag{3.31}$$

where variance process $v(t)$ is of square-Bessel CIR type [10].

The process is guaranteed to be positive if the Feller condition [16] for $v(t)$, i.e., $2\epsilon\bar{v} \geq \omega^2$, is satisfied.

It is shown in [10; 8] that, for a given time $t > 0$, $v(t)$ is distributed as $c(t)$ *times a non-central chi-squared random variable,* $\chi^2(d,\lambda(t))$*, with* d *the "degrees of freedom" parameter and non-centrality parameter* $\lambda(t)$, i.e.:

$$v(t) \sim c(t)\chi^2\left(d,\lambda(t)\right), \quad t > 0, \tag{3.32}$$

with

$$c(t) = \frac{1}{4\epsilon}\omega^2(1-\mathrm{e}^{-\epsilon t}), \quad d = \frac{4\epsilon\bar{v}}{\omega^2}, \quad \lambda(t) = \frac{4\epsilon v(0)\mathrm{e}^{-\epsilon t}}{\omega^2(1-\mathrm{e}^{-\epsilon t})}. \tag{3.33}$$

So, the corresponding cumulative distribution function (CDF) can be expressed as:

$$F_{v(t)}(x) = \mathbb{P}(v(t) \leq x) = \mathbb{P}\left(\chi^2\left(d, \lambda(t)\right) \leq x/c(t)\right) = F_{\chi^2(d,\lambda(t))}\left(x/c(t)\right), \tag{3.34}$$

where:

$$F_{\chi^2(d,\lambda(t))}(y) = \sum_{k=0}^{\infty} \exp\left(-\frac{\lambda(t)}{2}\right) \frac{\left(\frac{\lambda(t)}{2}\right)^k}{k!} \frac{\Gamma\left(k+\frac{d}{2}, \frac{y}{2}\right)}{\Gamma\left(k+\frac{d}{2}\right)}, \tag{3.35}$$

with

$$\Gamma(a,z) = \int_0^z t^{a-1}\mathrm{e}^{-t}\mathrm{d}t, \quad \Gamma(z) = \int_0^\infty t^{z-1}\mathrm{e}^{-t}\mathrm{d}t. \tag{3.36}$$

Further, the corresponding density function (see for example [33]) reads:

$$f_{\chi^2(d,\lambda(t))}(y) = \frac{1}{2}\mathrm{e}^{-\frac{1}{2}(y+\lambda(t))}\left(\frac{y}{\lambda(t)}\right)^{\frac{1}{2}\left(\frac{d}{2}-1\right)} \mathcal{B}_{\frac{d}{2}-1}(\sqrt{\lambda(t)y}), \tag{3.37}$$

with

$$\mathcal{B}_a(z) = \left(\frac{z}{2}\right)^a \sum_{k=0}^{\infty} \frac{\left(\frac{1}{4}z^2\right)^k}{k!\Gamma(a+k+1)}, \tag{3.38}$$

which is a modified Bessel function of the first kind (see for example [1; 20]).

The density for $v(t)$ can now be expressed as:

$$f_{v(t)}(x) \overset{def}{=} \frac{\mathrm{d}}{\mathrm{d}x}F_{v(t)}(x) = \frac{\mathrm{d}}{\mathrm{d}x}F_{\chi^2(d,\lambda(t))}(x/c(t)) = \frac{1}{c(t)}f_{\chi^2(d,\lambda(t))}\left(x/c(t)\right). \tag{3.39}$$

By using the properties of the non-central chi-square distribution the mean and variance of the process $v(t)$ are known explicitly:

$$\begin{aligned} \mathbb{E}(v(t)|v(0)) = &\quad c(t)(d+\lambda(t)), \\ \mathbb{V}\mathrm{ar}(v(t)|v(0)) = &\quad c^2(t)(2d+4\lambda(t)). \end{aligned} \tag{3.40}$$

In the lemma below we derive the corresponding expectation for $\sqrt{v(t)}$.

Lemma 3.2 (Expectation for $\sqrt{v(t)}$)**.** *For a given time $t > 0$ the expectation of $\sqrt{v(t)}$, where $v(t)$ has a non-central chi-square distribution function with CDF in (3.35), is given by:*

$$\alpha(t) := \mathbb{E}(\sqrt{v(t)}) = \sqrt{2c(t)}\mathrm{e}^{-\lambda(t)/2}\sum_{k=0}^{\infty}\frac{1}{k!}\left(\lambda(t)/2\right)^k \frac{\Gamma\left(\frac{1+d}{2}+k\right)}{\Gamma(\frac{d}{2}+k)}, \tag{3.41}$$

where $c(t)$, d and $\lambda(t)$ are defined in (3.33).

Proof. The proof can be found in Appendix A. □

3.4 Option Pricing and Hedging

3.4.1 European Options

European option prices can be obtained efficiently by use of the COS pricing method from [14], which is based on the availability of the characteristic function. The method employs a Fourier-cosine expansion of the density function.

From the general risk-neutral pricing formula the price of any European claim, $V(T, F(T))$, defined in terms of the underlying process, $F(T)$, can be written as:

$$\Pi(t, F(t)) = P(t,T)\mathbb{E}^T\left(V(T,F(T))|\mathcal{F}(t)\right) = P(t,T)\int_{\mathbb{R}} V(T,y)\widehat{f}_Y(y|x)\mathrm{d}y, \tag{3.42}$$

where $\widehat{f}_Y(y|x)$ is the transitional probability density function of F under the forward measure $\mathbb{Q}^T$.

Assuming fast decay of the density function, we can use the following approximation:

$$\Pi(t,x) \approx P(t,T) \int_{\delta_1}^{\delta_2} V(T,y) \widehat{f}_Y(y|x) \mathrm{d}y, \tag{3.43}$$

with $\delta_1 < \delta_2$. Now, in order to recover the density function $\widehat{f}_Y(y|x)$ one employs a Fourier cosine expansion based on the characteristic function:

$$\widehat{f}_Y(y|x) \approx \sum_{n=0}^{N} \frac{2\omega_n}{\delta_2 - \delta_1} \Re \left\{ \phi^T \left(kn, x(t), \tau\right) \mathrm{e}^{-ikn\delta_1} \right\} \cos(kn(y - \delta_1)), \tag{3.44}$$

with $\Re$ denoting taking the real part of the argument in brackets; $\phi^T(u, x(t), \tau)$ is defined in (3.21), $\omega_0 = 1/2$, $\omega_n = 1$, $n \in \mathbb{N}^+$ and $k = \pi/(\delta_2 - \delta_1)$. The transitional probability density function $\widehat{f}_Y(y|x)$ in Equation (3.42) is replaced by the cosine expansion:

$$\Pi(t,x) \approx P(t,T) \sum_{n=0}^{N} \omega_n \Re \left(\phi^T \left(kn, x(t), \tau\right) \mathrm{e}^{-ikn\delta_1} \right) \Gamma_n^{\delta_1, \delta_2}, \tag{3.45}$$

where the coefficients $\Gamma_n^{\delta_1,\delta_2}$ are known analytically for European options, see [14] for details and for error analysis regarding the different approximations.

The expansion in (3.45) exhibits an exponential convergence in the number of terms, N. Moreover, a whole vector of strikes can be priced simultaneously. A proper range of integration in (3.43) is a guarantee for fast convergence with only a few terms in the Fourier-cosine expansion. In [14], the integration range was based on the behavior of the probability density function. There, the choice was $\delta_1 = -L\sqrt{\tau}$ and $\delta_2 = L\sqrt{\tau}$, with $L = 8$. We use this integration range also here.

An important asset of the AH-G2++ model is the availability of the corresponding characteristic function so that we can calibrate the model fast and efficiently to plain vanilla contracts. We can also price certain exotic contracts, whose pricing can be related to the characteristic function. Moreover, Greeks can be derived easily for European contracts.

The Greeks determine the price sensitivities to changes in the underlying model parameters. We provide formulas for Delta, Δ, Gamma, Γ, and the sensitivities to the correlations, $\rho_{x,r}$, $\rho_{x,\zeta}$ and $\rho_{r,\zeta}$.

From the definition of a delta hedge we have:

$$\Delta := \frac{\partial \Pi(t,x)}{\partial S(t)} = \frac{\partial \Pi(t,x)}{\partial F(t)} \frac{\partial F(t)}{\partial S(t)} = \frac{1}{P(t,T)} \frac{\partial \Pi(t,x)}{\partial F(t)}.$$

With $u = kn$, the characteristic function of the AH-G2++ model reads:

$$\phi^T(kn, x(t), \tau) = \exp\left(ikn \log(F(t)) + \hat{C}(kn,\tau) v(t) + \hat{A}(kn,\tau) \right), \tag{3.46}$$

with $\hat{C}(kn,\tau)$ and $\hat{A}(kn,\tau)$ from (3.23), (3.24) and Equation (3.45), so that we have:

$$\Delta \approx \frac{1}{F(t)} \sum_{n=0}^{N} \omega_n \Re \Big\{ \phi^T \left(kn, x(t), \tau\right) \mathrm{e}^{-ikn\delta_1} ikn \Big\} \Gamma_n^{\delta_1,\delta_2}, \tag{3.47}$$

with $k = \pi/(\delta_2 - \delta_1)$.

For Gamma, $\Gamma = \dfrac{\partial \Delta}{\partial S}$ we find:

$$\Gamma \approx \frac{1}{P(t,T)} \frac{1}{F^2(t)} \sum_{n=0}^{N} \omega_n \Re \left\{ \phi^T \left(kn, x(t), \tau\right) \mathrm{e}^{-i\delta_1 kn} \Big((ikn)^2 - ikn \Big) \right\} \Gamma_n^{\delta_1,\delta_2}. \tag{3.48}$$

For the derivatives with respect to correlation, which we call [2] Rho(ρ), for $\rho = \{\rho_{x,r}, \rho_{x,\zeta}, \rho_{r,\zeta}\}$, we find:

$$\text{Rho}(\rho) := \frac{\partial}{\partial \rho}\Pi(t,x) \approx P(t,T)\sum_{n=0}^{N}\omega_n \Re\left\{\phi^T\left(kn, x(t), \tau\right)\mathrm{e}^{-i\delta_1 kn}\frac{\partial}{\partial\rho}\hat{A}(kn,\tau)\right\}\Gamma_n^{\delta_1,\delta_2}, \tag{3.49}$$

with $\hat{A}(kn,\tau)$ as in (3.46).

Depending on the different correlations, $\rho = \{\rho_{x,r}, \rho_{x,\zeta}, \rho_{r,\zeta}\}$, we determine the three partial derivatives $\frac{\partial}{\partial\rho}A(kn,\tau)$:

$$\begin{aligned}
\frac{\partial}{\partial\rho_{x,r}}\hat{A}(kn,\tau) &= \eta((kn)^2 + ikn)\int_0^\tau \mathbb{E}(\sqrt{v(T-s)})B(T-s,T)\mathrm{d}s,\\
\frac{\partial}{\partial\rho_{x,\zeta}}\hat{A}(kn,\tau) &= \gamma((kn)^2 + ikn)\int_0^\tau \mathbb{E}(\sqrt{v(T-s)})C(T-s,T)\mathrm{d}s,\\
\frac{\partial}{\partial\rho_{r,\zeta}}\hat{A}(kn,\tau) &= -\gamma\eta((kn)^2 + ikn)\int_0^\tau B(T-s,T)C(T-s,T)\mathrm{d}s,
\end{aligned}$$

with $B(t,T)$ defined in (2.17) and $C(t,T)$ in (2.18).

Here, we check the effect of correlations on the Greeks for a basic call option under the AH-G2++ model. We perform two experiments. First of all, in Figure 3.1(a), we show Δ, Γ, Rho($\rho_{x,r}$), Rho($\rho_{x,\zeta}$) and Rho($\rho_{r,\zeta}$). Secondly, in Figure 3.1(b) we vary the correlation between stock and the interest rate, $\rho_{x,r}$, and present the effect on Δ. In the experiments we consider a maturity of 15 years, $T = 15$, and the discount factor $P(0,T) = \exp(-0.06T)$ with the following set of parameters, $S(0) = 1$, $\epsilon = 0.3$, $\bar{v} = 0.02$, $\omega = 0.251$, $\kappa = 0.03$, $\eta = 0.02$, $\lambda = 1.1$ and $\gamma = 0.02$. The correlation structure is set as follows:

$$\begin{bmatrix} 1 & \rho_{x,v} & \rho_{x,r} & \rho_{x,\zeta} \\ * & 1 & 0 & 0 \\ * & * & 1 & \rho_{r,\zeta} \\ * & * & * & 1 \end{bmatrix} = \begin{bmatrix} 1 & -30\% & 20\% & 10\% \\ * & 1 & 0 & 0 \\ * & * & 1 & -90\% \\ * & * & * & 1 \end{bmatrix}. \tag{3.50}$$

The experiments indicate that when hedging these long-maturity European options,

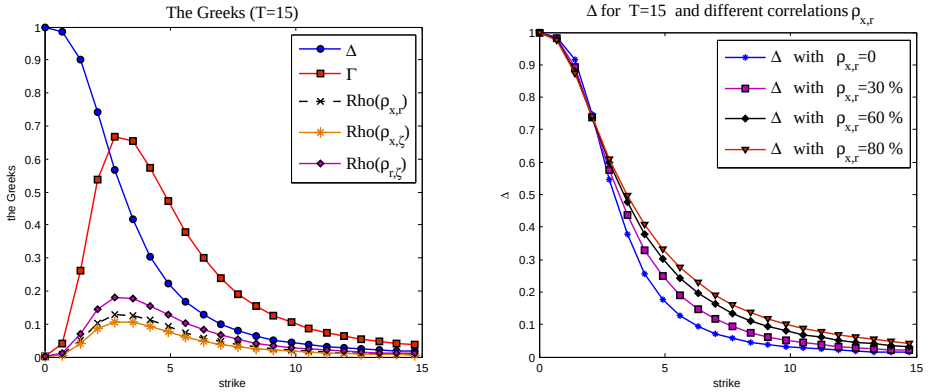

Figure 3.1: (a) Several Greek values for a call option. (b) Effect on delta of correlation, $\rho_{x,r}$, for a call option.

the correlation between stock and interest rates, $\rho_{x,r}$, has a significant effect on a delta hedge. Figure 3.1(b) also shows that if one assumes $\rho_{x,r} = 0$ and performs delta hedging a portfolio will be under/over hedged if the correlation is non-zero in reality.

In order to explain the increase of Δ as $\rho_{x,r}$ increases, we need to look at the underlying forward price, $F(t)$. The forward dynamics in Lemma 3.1 can be expressed

[2] not to confuse with the derivative with respect to interest rate in standard Black-Scholes model which is also called "rho".

as:

$$\frac{\mathrm{d}F(t)}{F(t)} = \sqrt{\Omega(t) - 2\rho_{x,r}\eta\mathbb{E}(\sqrt{v(t)})B(t,T)}\mathrm{d}W_F^T(t), \tag{3.51}$$

with

$$\begin{aligned}\Omega(t) &= v(t) + \gamma^2 C^2(t,T) + \eta^2 B^2(t,T) + 2\rho_{r,\zeta}\gamma\eta B(t,T)C(t,T) \\ &\quad -2\rho_{x,\zeta}\gamma\mathbb{E}(\sqrt{v(t)})C(t,T),\end{aligned} \tag{3.52}$$

and *another* Brownian motion $\mathrm{d}W_F^T(t)$.

Assuming that all the parameters stay constant, we analyze how the volatility term in front of $\mathrm{d}W_F(t)$ in (3.51) behaves for different correlations $\rho_{x,r}$. We find that for any set of parameters $\mathbb{E}(\sqrt{v(t)}) > 0$ and $B(t,T) \leq 0$. Therefore an increase of the correlation $\rho_{x,r}$ is directly related to an increase of the volatility of the forward. This explains the additional hedging costs presented in Figure 3.1(b) in presence of positive correlation between stock and the interest rate. The same pattern may be observed regarding $\rho_{x,\zeta}$ and $\rho_{r,\zeta}$.

3.4.2 Efficient Monte Carlo Simulation

Here, we briefly discuss an efficient Monte Carlo simulation scheme for the AH-G2++ model. We will adopt the algorithm by Andersen (see [3]), originally developed for the pure Heston stochastic volatility model.

As presented in Lemma 3.1 the AH-G2++ (as well as the H-G2++) model can formulated as:

$$\begin{aligned}\frac{\mathrm{d}F(t)}{F(t)} &= \hat{\psi}_1(t)\mathrm{d}\widetilde{W}_r^T(t) + \hat{\psi}_2(t)\mathrm{d}\widetilde{W}_\zeta^T(t) + \rho_{x,v}\sqrt{v(t)}\mathrm{d}\widetilde{W}_v^T(t) \\ &\quad + \sqrt{v(t)\left(1-\rho_{x,v}^2\right) + \psi_5(t)}\mathrm{d}\widetilde{W}_x^T(t), \qquad (3.53) \\ \mathrm{d}v(t) &= \epsilon(\bar{v} - v(t))\mathrm{d}t + \omega\sqrt{v(t)}\mathrm{d}\widetilde{W}_v^T(t), \qquad (3.54)\end{aligned}$$

with

$$\begin{aligned}\hat{\psi}_1(t) &= \mathbf{U}_{4,1}\alpha(t) - (\rho_{r,\zeta}\gamma C(t,T) + \eta B(t,T)), \\ \hat{\psi}_2(t) &= \mathbf{U}_{4,2}\alpha(t) - \gamma C(t,T)\sqrt{1-\rho_{r,\zeta}^2}, \\ \psi_5(t) &= -\alpha^2(t)\left(\mathbf{U}_{4,1}^2 + \mathbf{U}_{4,2}^2\right),\end{aligned}$$

and $\mathbf{U}_{4,1}$, $\mathbf{U}_{4,2}$ are defined in (3.4). We have $\alpha(t) = \mathbb{E}(\sqrt{v(t)})$ for the AH-G2++ model (and $\alpha(t) = \sqrt{v(t)}$ for the H-G2++ model). Since the difference between the AH-G2++ and the H-G2++ model appears only in function $\alpha(t)$ the Monte Carlo schemes are very similar.

In both models the dynamics for the forward, $F(t)$, do not depend on the interest rate processes, $r(t)$ or $\zeta(t)$. This implies that for Monte Carlo paths for $F(t)$ only the 2D stochastic differential equations for the forward, $F(t)$, and its variance process, $v(t)$, need to be discretized.

Since the Brownian motions in the models are independent, we can perform a simplifying factorization,

$$\begin{aligned}\frac{\mathrm{d}F(t)}{F(t)} &= \sqrt{\hat{\psi}_1^2(t) + \hat{\psi}_2^2(t) + v(t)\left(1-\rho_{x,v}^2\right) + \psi_5(t)}\mathrm{d}\widetilde{W}_F^T(t) + \rho_{x,v}\sqrt{v(t)}\mathrm{d}\widetilde{W}_v^T(t), \\ \mathrm{d}v(t) &= \epsilon(\bar{v} - v(t))\mathrm{d}t + \omega\sqrt{v(t)}\mathrm{d}\widetilde{W}_v^T(t),\end{aligned}$$

with $\mathrm{d}\widetilde{W}_F^T(t)$ independent of $\mathrm{d}\widetilde{W}_v^T(t)$.

In log-transformed coordinates, $x(t) = \log F(t)$, we find with Itô's Lemma:

$$\mathrm{d}x(t) = \frac{1}{2}\left(\chi(t,T) - v(t)\right)\mathrm{d}t + \sqrt{\xi(t,v(t))}\mathrm{d}\widetilde{W}_F^T(t) + \rho_{x,v}\sqrt{v(t)}\mathrm{d}\widetilde{W}_v^T(t), \tag{3.55}$$

with $\xi(t,v(t)) = -\chi(t,T) + v(t) - \rho_{x,v}^2 v(t)$, where

$$\begin{aligned}\chi(t,T) &:= -\gamma^2 C^2(t,T) - \eta^2 B^2(t,T) - 2\rho_{r,\zeta}\gamma\eta B(t,T)C(t,T) \\ &\quad +2\alpha(t)\Big(\rho_{x,r}\eta B(t,T) + \rho_{x,\zeta}\gamma C(t,T)\Big),\end{aligned} \tag{3.56}$$

with $\alpha(t) = \sqrt{v(t)}$ for the H-G2++ model or $\alpha(t) = \mathbb{E}(\sqrt{v(t)})$ for the AH-G2++ model.

The variance process $v(t)$ is also independent of the interest rates processes, $r(t)$ and $\zeta(t)$:

$$\mathrm{d}v(t) = \epsilon(\bar{v} - v(t))\mathrm{d}t + \omega\sqrt{v(t)}\mathrm{d}\widetilde{W}_v^T(t). \tag{3.57}$$

For $t > 0$, $v(t)$ is from a non-central chi-square distribution [10]. The direct sampling of $v(t)$ can be very efficiently performed with the Quadratic Exponential (QE) scheme proposed in [3].

In order to obtain a bias-free scheme (see [8]) for sampling the forward price process, it is convenient to first integrate the SDE for $v(t)$, i.e:

$$v(t+\delta) = v(t) + \int_t^{t+\delta} \epsilon(\bar{v} - v(s))\mathrm{d}s + \omega\int_t^{t+\delta}\sqrt{v(s)}\mathrm{d}\widetilde{W}_v^T(s). \tag{3.58}$$

Process $x(t)$ from (3.55) can be expressed in integral form as:

$$\begin{aligned}x(t+\delta) &= x(t) + \frac{1}{2}\int_t^{t+\delta}\left(\chi(s,T) - v(s)\right)\mathrm{d}s + \int_t^{t+\delta}\sqrt{\xi(s,v(s))}\mathrm{d}\widetilde{W}_F^T(s) \\ &\quad +\rho_{x,v}\int_t^{t+\delta}\sqrt{v(s)}\mathrm{d}\widetilde{W}_v^T(s).\end{aligned} \tag{3.59}$$

The last integral in (3.59) can easily be determined by Equation (3.58). In the discretization (3.59) we distinguish the time and stochastic-type integrals. Those integrals can be handled as indicated in [3]. For a state-dependent function $f(t,v(t))$ the time integrals can be approximated by

$$\int_t^{t+\delta} f(t,v(s))\mathrm{d}s \approx \delta\left(\gamma_1 f(t,v(t)) + \gamma_2 f(t+\delta, v(t+\delta))\right), \tag{3.60}$$

with certain weights γ_1 and γ_2. For the stochastic integrals we have, with help of Itô's Isometry,

$$\int_t^{t+\delta}\sqrt{\xi(s,v(s))}\mathrm{d}\widetilde{W}_F^T(s) \sim \mathcal{N}\left(0, \int_t^{t+\delta}\xi(s,v(s))\mathrm{d}s\right), \tag{3.61}$$

with $\mathcal{N}(a,b)$ indicating a normal distribution with mean a and variance b.

We note that an extension from a 2-factor interest rate process to n factors is trivial, since only the functions $\chi(s,T)$ and $\xi(s,v(s))$ then consist of more terms.

The scheme developed will be used in a number of experiments in the next sections.

4 Numerical Experiments

In this section we compare prices obtained by the AH-G2++ model with those by the Schöbel-Zhu-Hull-White model and by the H-G2++ model. We use European options, and also check the performance of the hybrid models when pricing an exotic hybrid derivative in the final subsection.

4.1 Comparison with Schöbel-Zhu Model

Here, we compare the AH-Gn++ model to the Schöbel-Zhu model with Gaussian interest rates. The Schöbel-Zhu model is driven by the SDEs:

$$\begin{cases}\mathrm{d}\widetilde{x}(t) = & \left(r(t) - \frac{1}{2}\sigma^2(t)\right)\mathrm{d}t + & \sigma(t)\mathrm{d}W_{\widetilde{x}}(t), \\ \mathrm{d}\sigma(t) = & \widetilde{\epsilon}\left(\bar{\sigma} - \sigma(t)\right)\mathrm{d}t + & \widetilde{\omega}\mathrm{d}W_\sigma(t),\end{cases} \tag{4.1}$$

with $\mathrm{d}W_{\widetilde{x}}(t)\mathrm{d}W_{\sigma}(t) = \rho_{\widetilde{x},\sigma}\mathrm{d}t$ and positive parameters. The stochastic volatility model by Heston (as for the AH-Gn++ model) has the following dynamics:

$$\begin{cases} \mathrm{d}x(t) = & \left(r(t) - \frac{1}{2}v(t)\right)\mathrm{d}t + & \sqrt{v(t)}\mathrm{d}W_x(t), \\ \mathrm{d}v(t) = & \epsilon\left(\bar{v} - v(t)\right)\mathrm{d}t + & \omega\sqrt{v(t)}\mathrm{d}W_v(t), \end{cases} \tag{4.2}$$

with positive parameters and the correlation $\mathrm{d}W_x(t)\mathrm{d}W_v(t) = \rho_{x,v}\mathrm{d}t$. For both models the interest rate process $r(t)$ is identical, driven by a correlated, normally distributed, short-rate model, so that we only need to focus on a differences in the volatility processes.

The volatility in the Schöbel-Zhu model is driven by a normally distributed Ornstein-Uhlenbeck process $\sigma(t)$, whereas in the Heston model the volatility is $\sqrt{v(t)}$ with $v(t)$ distributed as $c(t)$ times a non-central chi-squared random variable, $\chi^2(d, \lambda(t))$, as discussed in Subsection 3.3.

We determine under which conditions the two volatility processes, for the Schöbel-Zhu, $\sigma(t)$, and for the Heston model, $\sqrt{v(t)}$, coincide. In other words: we determine under which conditions $\sqrt{v(t)}$ is approximately a normal distribution (as $\sigma(t)$ in the Schöbel-Zhu model is normally distributed).

Result 4.1 ($\sqrt{v(t)}$ as a normal distribution for $0 < t < \infty$)**.** *For $t < \infty$, the square root of $v(t)$ in (4.2) can be approximated by*

$$\sqrt{v(t)} \approx \mathcal{N}\left(\sqrt{c(t)(\lambda(t)-1) + c(t)d + \frac{c(t)d}{2(d+\lambda(t))}}, c(t) - \frac{c(t)d}{2(d+\lambda(t))}\right), \tag{4.3}$$

with $c(t)$, d and $\lambda(t)$ from (3.33). Moreover, for a fixed value of z in the cumulative distribution function $F_{\sqrt{v(t)}}(z)$, and a fixed value for parameter, d, the error is of order $\mathcal{O}(\lambda^2(t))$ for $\lambda(t) \to 0$ and $\mathcal{O}(1/\sqrt{\lambda(t)})$ for $\lambda(t) \to \infty$.

As already indicated in [35] the normal approximation (4.3) is a satisfactory approximation for either a large number of degrees of freedom, d, or a large non-centrality parameter $\lambda(t)$. A large number of degrees of freedom, $d \gg 0$, implies that $4\epsilon\bar{v} \gg \omega^2$, which is closely related to the Feller condition, $2\epsilon\bar{v} > \omega^2$. The Heston model thus has a similar volatility structure as the Schöbel-Zhu model when the Feller condition is satisfied.

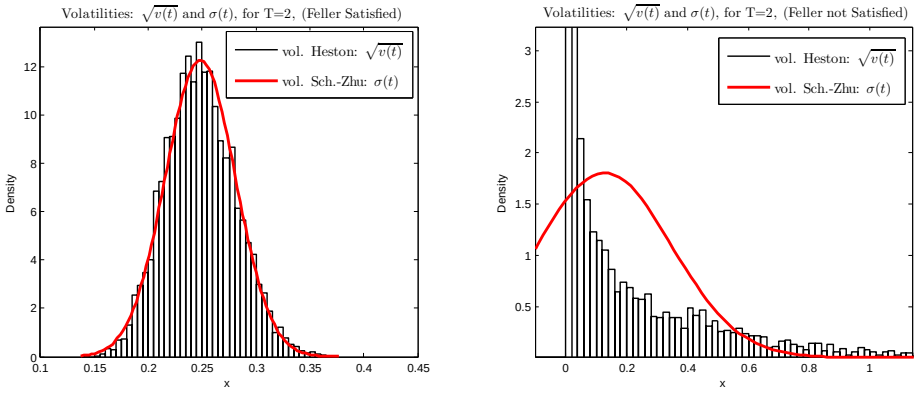

Figure 4.1: Histogram for $\sqrt{v(t)}$ (the Heston model) and density for $\sigma(t)$ (the Schöbel-Zhu model); Maturity $T = 2$. LEFT: Feller condition satisfied $\kappa = 1.2$, $v(0) = \bar{v} = 0.0625$, $\gamma = 0.1$; RIGHT: The Feller condition violated $\kappa = 0.25$, $v(0) = \bar{v} = 0.0625$, $\gamma = 0.625$ as in [4].

Figure 4.1 confirms this observation. The volatilities for the Heston and Schöbel-Zhu models differ significantly when the Feller condition does not hold as the volatility in the Heston model gives rise to much heavier tails than those in the Schöbel-Zhu model. This may have a significant effect when calibrating the models to the market data with significant implied volatility smile or skew.

4.1.1 Calibration of the Hybrid Models

Here we examine the two models and check their performance when calibration to real market data. The Schöbel-Zhu-Hull-White and the AH-G1++ models (i.e. affine Heston with Hull-White short-rate process) are calibrated to implied volatilities from the S&P500 (27/09/2010) [3] with spot price at 1145.88.

Firstly, we calibrate the parameters for the interest rate process by using caplets and swaptions. Standard procedures for the Hull-White calibration are employed [7]. Secondly, the remaining parameters, for the underlying asset, the equity volatility and the correlations, are calibrated to the plain vanilla equity options.

For both models the correlation between the stock and interest rates, $\rho_{x,r}$, is set to +30%.

		Implied Volatility [%]			Error [%]	
T	Strike	Market	SZHW	AH-G1++	err.(SZHW)	err.(AG-G1++)
T=6m	40%	57.61	54.02	57.05	3.59 %	-0.56 %
	80%	31.38	34.33	33.22	-2.95 %	1.84 %
	100%	22.95	25.21	21.57	-2.26 %	-1.38 %
	120%	15.9	18.80	16.38	-2.90 %	0.48 %
	180%	24.54	22.60	24.40	1.94 %	-0.14 %
T=1y	40%	48.53	47.01	48.21	1.52 %	0.32 %
	80%	30.37	31.69	31.07	-1.32 %	-0.70 %
	100%	24.49	24.97	24.28	-0.48 %	0.21 %
	120%	19.23	19.09	19.14	0.14 %	0.09 %
	180%	18.42	18.28	18.40	0.14 %	0.02 %
T=5y	40%	41.30	40.00	41.20	1.30 %	0.10 %
	80%	31.12	31.88	31.38	-0.76 %	-0.26 %
	100%	27.83	28.75	27.86	-0.92 %	-0.03 %
	120%	25.13	25.93	24.91	-0.80 %	0.22 %
	180%	19.28	18.57	19.32	0.71 %	-0.04 %
T=10y	40%	36.76	36.15	36.75	0.61 %	0.01 %
	80%	31.04	31.25	31.08	-0.21 %	-0.04 %
	100%	29.18	29.47	29.18	-0.29 %	0.00 %
	120%	27.66	27.93	27.62	-0.27 %	0.04 %
	180%	24.34	24.15	24.35	0.19 %	-0.01 %

Table 4.1: Calibration results for the Schöbel-Zhu hybrid model (SZHW) and the AH-G1++ hybrid.

The calibration results, presented in Table 4.1, confirm that the AH-G1++ model is more *flexible* than the Schöbel-Zhu-Hull-White model. The difference is pronounced for large strikes for which the error for the affine Heston hybrid model is up to 20 times lower than for the Schöbel-Zhu-Hull-White hybrid model.

4.2 The AH-G2++ and the H-G2++ Models for Pricing Long-term Maturity Options

In the second experiment we check the performance of the H-G2++ model against its affine sister, the AH-G2++ model pricing plain vanilla options.

First of all, we generate European call prices with the H-G2++ hybrid model by a Monte Carlo simulation (from Section 3.4.2). Secondly, we compare, in terms of implied volatilities, with results from the AH-G2++ hybrid model obtained by the COS method. We consider two cases, one in which the model parameters satisfy the Feller condition for the stock and another experiment in which they do not satisfy this condition.

Experiment 4.2 (Feller's condition satisfied, $2\epsilon\bar{v} \geq \omega^2$)**.** We compare the results of the H-G2++ and AH-G2++ models. The parameters are chosen as:

$$\epsilon = 0.8 \;\; \bar{v} = 0.2, \;\; \omega = 0.2, \;\; \kappa = 1.1, \;\; \eta = 0.01, \;\; \lambda = 0.8, \;\; \gamma = 0.015,$$

[3] dataset obtained from Rabobank International.

and the correlation is given by:

$$\begin{bmatrix} 1 & \rho_{x,v} & \rho_{x,r} & \rho_{x,\zeta} \\ * & 1 & \rho_{v,r} & \rho_{v,\zeta} \\ * & * & 1 & \rho_{r,\zeta} \\ * & * & * & 1 \end{bmatrix} = \begin{bmatrix} 1 & -30\% & 35\% & 8\% \\ * & 1 & 0\% & 0\% \\ * & * & 1 & -40\% \\ * & * & * & 1 \end{bmatrix}. \tag{4.4}$$

The initial conditions are $S(0) = 1$ and $v(0) = \bar{v}$ with the initial yield given by $P(0,T) = \exp(-0.03T)$. With these parameters the Feller condition for the stock is satisfied. We choose four maturities $\tau = 1$, $\tau = 5$, $\tau = 10$ and $\tau = 20$. Table 4.2 shows an almost perfect correspondence between the volatilities.

Implied Volatility [%]				
T	Strike	H-G2++ (MC)	AH-G2++ (Fourier)	difference
1y	0.8869	44.81 (0.19)	44.79	-0.02 %
	0.9324	44.67 (0.23)	44.65	-0.02 %
	1.0305	44.40 (0.30)	44.38	-0.02 %
	1.1388	44.16 (0.38)	44.13	-0.03 %
	1.1972	44.04 (0.42)	44.01	-0.03 %
5y	0.8308	44.59 (0.11)	44.60	0.01 %
	0.9290	45.07 (0.12)	45.07	0.01 %
	1.1618	37.89 (0.15)	37.89	0.00 %
	1.4530	30.86 (0.23)	30.85	-0.01 %
	1.6248	27.52 (0.25)	27.50	-0.02 %
10y	0.8400	44.57 (0.09)	44.54	-0.02 %
	0.9839	44.44 (0.13)	44.42	-0.02 %
	1.3499	44.22 (0.25)	44.20	-0.02 %
	1.8519	44.00 (0.40)	43.99	0.02 %
	2.1692	43.90 (0.48)	43.88	0.01 %
20y	0.9316	44.55 (0.18)	44.49	-0.05 %
	1.1651	44.46 (0.22)	44.40	-0.06 %
	1.8221	44.31 (0.38)	44.24	-0.07 %
	2.8497	44.16 (0.45)	44.07	-0.08 %
	3.5638	44.08 (0.52)	44.00	-0.08 %

Table 4.2: Difference in implied volatilities between the H-G2++ (simulated with Monte Carlo) and the AH-G2++ (COS method). Numbers in brackets indicate standard deviations. The simulation was performed with Feller's condition satisfied.

Experiment 4.3 (Feller's condition violated, $2\epsilon\bar{v} \leq \omega^2$)**.** In practice there are many cases in which the Feller condition is not satisfied. Therefore we check the performance of the affine hybrid model in such a setup. In this experiment we choose $\epsilon = 0.4$, $\bar{v} = 0.2$ and $\omega = 0.6$ and the remaining parameters are as in Experiment 4.2. The Feller condition does not hold in this case, as $0.16 \not\geq 0.36$. Therefore, the probability of hitting zero is positive. Table 4.3 shows that our tractable hybrid model, the AH-G2++, provides values close to the H-G2++ model.

These experiments, with standard parameters, show that the results of the AH-G2++ model resemble the results of the H-G2++ very well.

Remark. The AH-Gn++ and the H-Gn++ models differ only in the definition of function $\alpha(t)$ in the associated covariance matrix. This $\alpha(t)$ is multiplied either by $\rho_{x,r}\eta$ or by $\rho_{x,\zeta}\gamma$. It is therefore evident that both models produce very similar results when either the correlations or the volatilities for the interest rates, γ, η, are *small*. Obviously the correlations are, by definition, bounded by 1. The volatilities for the short-rate models are on the other hand typically also of small size (values < 0.1 are often reported in the literature [7]). In the experiments to follow we check the model performance for unrealistically high volatilities to stress the proposed AH-G2++ model.

4.3 Pricing of a Hybrid Product

In this test we consider an equity-interest rate diversification hybrid product. This product is based on sets of assets with different expected returns and risk levels. Proper

Implied Volatility [%]				
T	Strike	H-G2++ (MC)	AH-G2++ (Fourier)	difference
1y	0.8869	43.12 (0.15)	43.17	0.05 %
	0.9324	42.53 (0.16)	42.58	0.05 %
	1.0305	41.48 (0.16)	41.54	0.06 %
	1.1388	40.71 (0.20)	40.76	0.04 %
	1.1972	40.44 (0.26)	40.48	0.04 %
5y	0.8308	40.29 (0.08)	40.26	-0.03 %
	0.9290	39.59 (0.09)	39.54	-0.05 %
	1.1618	38.40 (0.13)	38.33	-0.08 %
	1.4530	37.59 (0.17)	37.48	-0.11 %
	1.6248	37.33 (0.17)	37.22	-0.11 %
10y	0.8400	39.82 (0.14)	39.71	-0.11 %
	0.9839	39.22 (0.17)	39.11	-0.11 %
	1.3499	38.17 (0.23)	38.06	-0.11 %
	1.8519	37.37 (0.35)	37.28	-0.10 %
	2.1692	37.09 (0.40)	37.01	-0.08 %
20y	0.9316	39.71 (0.06)	39.60	-0.11 %
	1.1651	39.24 (0.06)	39.13	-0.11 %
	1.8221	38.40 (0.15)	38.29	-0.11 %
	2.8497	37.73 (0.30)	37.62	-0.11 %
	3.5638	37.48 (0.41)	37.36	-0.12 %

Table 4.3: Difference in implied volatilities between the H-G2++ (simulated with Monte Carlo) and the AH-G2++ (COS method). Numbers in brackets indicate standard deviations. The simulation was performed with Feller's condition violated.

construction of such a product may give reduced risk compared to any single asset, and an expected return that is greater than that of the least risky asset [28]. A basic example is a portfolio with two assets: a stock with a high risk and high return and a zero-coupon bond with a low risk and low return. If one introduces an equity component in a zero-coupon bond portfolio the expected return will increase. However, because of a non-perfect correlation between these two assets also a risk reduction is expected. If the percentage of the equity in the portfolio is increased, it eventually starts to dominate the structure and the risk may increase with a higher impact for a low or negative correlation. The example is defined as follows:

$$\text{payoff} = \max\left(\hat{w}_1 S(T_1) + \hat{w}_2 P(T_1, T), 0\right), \tag{4.5}$$

where for $T_1 < T$, $S(T_1)$ is the underlying asset at time T_1, $P(T_1, T)$ is a zero-coupon bond and which pays €1 at time T and $\hat{w}_1$ and $\hat{w}_2$ are weighting factors, which can be either positive (in a long-position) or negative (in a short position).

The value of the contract in (4.5), at time t, under the risk-neutral measure $\mathbb{Q}$, can be expressed by:

$$\Pi(t, S(t)) = \mathbb{E}^{\mathbb{Q}}\left(\frac{1}{M(T_1)} \max\left(\hat{w}_1 S(T_1) + \hat{w}_2 P(T_1, T), 0\right) \Big| \mathcal{F}(t)\right). \tag{4.6}$$

Since the expectation in (4.6) contains a correlated stock, a zero-coupon bond, and the money-savings account this expectation is difficult to determine analytically.

However, by a change of numéraire, from the money-savings account, to a zero coupon bond maturing at time T the expectation in (4.6) simplifies significantly.

The Radon-Nikodým derivative is known as:

$$\frac{\mathrm{d}\mathbb{Q}^T}{\mathrm{d}\mathbb{Q}}\Big|_{\mathcal{F}(T_1)} = \frac{1}{M(T_1)} \frac{P(T_1, T)}{P(0, T)}. \tag{4.7}$$

So, the price in (4.6) under the $T-$forward measure, $\mathbb{Q}^T$, reads:

$$\Pi(t, S(t)) = P(0, T)\mathbb{E}^T\left(\frac{1}{P(T_1, T)} \max\left(\hat{w}_1 S(T_1) + \hat{w}_2 P(T_1, T), 0\right) \Big| \mathcal{F}(t)\right). \tag{4.8}$$

Since the forward $F(t)$ is defined as $F(t) = S(t)/P(t,T)$ the expectation above reduces to:

$$\Pi(t, S(t)) = P(0,T)\mathbb{E}^T\left(\max\left(\hat{w}_1 F(T_1) + \hat{w}_2, 0\right)\Big|\mathcal{F}(t)\right). \tag{4.9}$$

We recognize that the Expectation (4.9) is a call option with strike $K = -\hat{w}_2$ and a constant multiplier, $\hat{w}_1$.

Since we consider the affine Heston hybrid model, AH-G2++ here, we can simply determine the price of (4.9) by the COS method described in Section 3.4. The evaluation of such a payoff can be evaluated in a split-second.

We now perform the experiment in which we compare the performance of the H-G2++ and the AH-G2++ models for this hybrid product. For $T_1 = 5$ and $T = 8$ we choose the following set of parameters [4]: $\epsilon = 0.25$, $\bar{v} = v(0) = 0.0625$, $\omega = 0.625$, $\kappa = 0.05$, $\eta = 0.03$, $\lambda = 0.4$, $\gamma = 0.05$, $\rho_{x,v} = -30\%$ and $\rho_{r,\zeta} = -20\%$. The zero-coupon bond $P(0,T) = \exp(-0.03T)$ and $\rho_{x,r} = \rho_{x,\zeta}$. The prices for the hybrid product $\Pi(t, S(t))$ in (4.9) are calculated for different correlations between stock and the interest rate, $\rho_{x,r}$. For the payoff we take $\hat{w}_1 = 1$ and $\hat{w}_2 = \{-4, \ldots, 0\}$ and compute Monte Carlo prices with 100.000 paths and $10T_1$ time-steps for the H-G2++ model and by the Fourier expansion for the AH-G2++ model. The output is presented in Figure 4.2(a).

In Figure 4.2(b) the results for an extreme parameter setting are presented. In this experiment we have taken a high volatility for the interest rates $\eta = 0.25$ (whereas typically $\eta, \gamma < 0.025$ as presented in [7]). We report that for such an extreme parameter set the AH-G2++ model provides results which agree rather well with those obtained by the H-G2++ model. This is another indication of the highly satisfactory performance of AH-G2++.

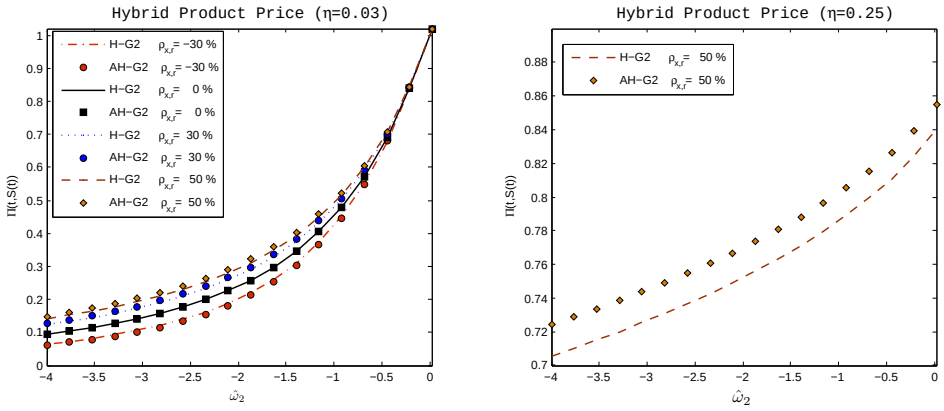

Figure 4.2: Prices generated by the H-G2++ and the AH-G2++ models. LEFT: results for $\eta = 0.03$, RIGHT: results for $\eta = 0.25$.

5 Conclusions and Final Remarks

In this article we have constructed an equity-interest rate hybrid model with non-zero correlation between the asset classes. The model is in the class of affine diffusion processes so that we can determine a closed-form characteristic function. Availability of a characteristic function is crucial for efficient model calibration to plain vanilla options. By defining the affine hybrid Heston model under the forward measure, we can price several financial derivative products as under the basic Heston model.

For the affine Heston-Gaussian multi-factor model, AH-Gn++, we have discussed an efficient Monte Carlo simulation scheme and an effective way for calculating the Greeks of plain vanilla options.

[4] The stochastic volatility parameters are chosen as in [4].

We have also shown that the AH-Gn++ model provides derivative prices similar to the (non-affine) Heston-Gaussian multi-factor (H-Gn++) model and superior to Schöbel-Zhu variants if the Feller condition is violated.

Acknowledgments

The authors would like to thank Natalia Borovykh from Rabobank International for fruitful discussions and helpful comments.

References

[1] M. Abramowitz, I.A. Stegun, Modified Bessel Functions **I** and **K**, *Handbook of Mathematical Functions with Formulas, Graphs, and Mathematical Tables, 9th ed. New York: Dover,* 374-377, 1972.

[2] R. Ahlip and M. Rutkowski, Forward Start Options in Heston's Model Under Stochastic Interest Rates. *IJTAF,* 12: 209-225, 2009.

[3] L. Andersen, Simple and Efficient Simulation of the Heston Stochastic Volatility Model. *Comp. Fin.*, 11(3): 1-42, 2008.

[4] A. Antonov, M. Arneguy and N. Audet, Markovian Projection to a Displaced Volatility Heston Model. SSRN working paper, 2008. Available at SSRN: `http://ssrn.com/abstract=1106223`.

[5] F. Black and M. Scholes, The Pricing of Options and Corporate Liabilities. *J. Political Economy,* 81: 637–654, 1973.

[6] M. Bouzoubaa and A. Osseiran, *Exotic Options and Hybrids. A Guide to Structuring, Pricing and Trading.* Willey Finance, United Kingdom, 2010.

[7] D. Brigo and F. Mercurio, *Interest Rate Models- Theory and Practice: With Smile, Inflation and Credit.* Springer Finance, 2nd ed., 2007.

[8] M. Broadie and Ö. Kaya, Exact Simulation of Stochastic Volatility and other Affine Jump Diffusion Processes. *Operations Research,* 54: 217–231, 2006.

[9] P.P. Carr and D.B. Madan, Option Valuation Using the Fast Fourier Transform. *J. Comp. Finance,* 2:61-73, 1999.

[10] J.C. Cox, J.E. Ingersoll and S.A. Ross, A Theory of the Term Structure of Interest Rates. *Econometrica* 53: 385-407, 1985.

[11] D. Duffie, J. Pan and K. Singleton, Transform Analysis and Asset Pricing for Affine Jump-Diffusions. *Econometrica,* 68: 1343–1376, 2000.

[12] D.J. Duffy, *Finite Difference Methods in Financial Engineering. A partial Differential Equation Approach.* John Wiley & Sons, Ltd, 2006.

[13] D. Dufresne, The Integrated Square-Root Process. Working paper, University of Montreal, 2001. Available at: `http://en.scientificcommons.org/35755469`.

[14] F. Fang and C.W. Oosterlee, A Novel Pricing Method for European Options Based on Fourier-Cosine Series Expansions. *SIAM J. Sci. Comput.*, 31: 826, 2008.

[15] F. Fang and C.W. Oosterlee, Pricing Options under Stochastic Volatility with Fourier Cosine Expansions. *Techn. Report*, Delft University of Technology, Delft, the Netherlands, 2010. Submitted for publication.

[16] W. Feller, *An Introduction to Probability Theory and its Applications,* Volume 2, 2nd ed., Wiley, Chicester, 1971.

[17] C. He, J.S. Kennedy, T. Coleman, P.A. Forsyth, Y. Li and K. Vetzal, Calibration and Hedging Under Jump Diffusion. *Review of Derivatives Research* 9: 1–35, 2006.

[18] J. Gatheral, *The Volatility Surface. A Practitioner's Guide.* John Wiley & Sons, Ltd, 2006.

[19] H. Geman, N. El Karoui and J.C. Rochet, Changes of Numéraire, Changes of Probability Measures and Pricing of Options. *J. Appl. Prob.* 32: 443–458, 1995.

[20] I.S. Gradshteyn and I.M. Ryzhik, *Table of Integrals, Series, and Products*, 5th ed., A. Jeffrey, Ed. Academic Press, San Diego, 1996.

[21] L.A. Grzelak and C.W. Oosterlee, On the Heston Model with Stochastic Interest Rates. *Forthcoming in SIAM J. Finan. Math.*, 2011. Available at SSRN: `http://ssrn.com/abstract=1382902`.

[22] L.A. Grzelak, C.W. Oosterlee and S.v. Weeren, Extension of Stochastic Volatility Equity Models with Hull-White Interest Rate Process. *Quant. Fin.*, 1469-7696, 2009.

[23] L.A. Grzelak and C.W. Oosterlee, An Equity-Interest Rate Hybrid Model with Stochastic Volatility and Interest Rate Smile. *Submited for publication.*

Techn. Report 10-01, Delft Univ. Techn., the Netherlands. Available at SSRN: http://ssrn.com/abstract=1543704.
[24] S.L. Heston, A Closed-Form Solution for Options with Stochastic Volatility with Applications to Bond and Currency Options. *Rev. Finan. Stud.,* 2(6): 327–343, 1993.
[25] J. Hull, Interest Rate Derivatives: Models of the Short Rate. *Option, Futures, and Other Derivatives,* 6: 657-658, 2006.
[26] J. Hull, *Options, Futures, and Other Derivatives, 7th ed.* Prentice Hall, 2008.
[27] J. Hull and A. White, Using Hull-White Interest Rate Trees, *J. Derivatives,* 4: 26–36, 1996.
[28] C. Hunter and G. Picot, *Hybrid Derivatives- Financial Engines of the Future.* The Euromoney- Derivatives and Risk Management Handbook, BNP Paribas, 2005/06.
[29] E.E. Kummer, Über die Hypergeometrische Reihe $F(a;b;x)$. *J. reine angew. Math.,* 15: 39–83, 1936.
[30] W. Koepf, *Hypergeometric Summation: An Algorithmic Approach to Summation and Special Function Identities.* Braunschweig, Germany: Vieweg, 1998.
[31] R. Lord, R. Koekkoek and D. van Dijk, A Comparison of Biased Simulation Schemes for Stochastic Volatility Models. *Quant. Fin.,* 10(2): 171–194, 2010.
[32] K.W. Morton and D.F. Mayers, *Numerical Solution of Partial Differential Equations-An Introduction.* Cambridge University Press, 2005.
[33] S.M. Moser, Some Expectations of a Non-Central Chi-Square Distribution with an Even Number of Degrees of Freedom, *TENCON 2007 - 2007 IEEE Region 10 Conference*, Oct. 30 2007-Nov. 2 2007.
[34] M. Musiela and M. Rutkowski, *Martingale Methods in Financial Modelling.* Springer Finance, 1997.
[35] P.B. Patnaik, The Non-Central χ^2 and F-Distributions and their Applications. *Biometrika,* 36: 202-232, 1949.
[36] L.C.G. Rogers, Which Model for Term-Structure of Interest Rates Should One Use? *Math. Fin.,* 65: 93-115, 1995.
[37] R. Schöbel and J. Zhu, Stochasic Volatility with an Ornstein-Uhlenbeck Process: An extension. *Europ. Fin. Review*, 3:23–46, 1999.
[38] A.van Haastrecht, R. Lord, A. Pelsser and D. Schrager, Pricing Long-Maturity Equity and FX Derivatives with Stochastic Interest Rates and Stochastic Volatility. *Ins.: Mathematics Econ.,* 45(3), 436–448, 2009.

A Proof of Lemma 3.2

Proof. First of all by [13] we have that:

$$\begin{aligned}\mathbb{E}(\sqrt{v(t)}|v(0)) &:= \int_0^\infty \frac{\sqrt{x}}{c(t)} f_{\chi^2(d,\lambda(t))}\left(\frac{x}{c(t)}\right)\mathrm{d}x \\ &= \sqrt{2c(t)}\frac{\Gamma\left(\frac{1+d}{2}\right)}{\Gamma\left(\frac{d}{2}\right)}{}_1F_1\left(-\frac{1}{2},\frac{d}{2},-\frac{\lambda(t)}{2}\right), \qquad \text{(A.1)}\end{aligned}$$

where ${}_1F_1(a;b;z)$ is a confluent hyper-geometric function, which is also known as Kummer's function [29] of the first kind, given by:

$${}_1F_1(a;b;z) = \sum_{k=0}^{\infty}\frac{(a)_k}{(b)_k}\frac{z^k}{k!}, \qquad \text{(A.2)}$$

with $(a)_k$ and $(b)_k$ being Pochhammer symbols of the form:

$$(a)_k = \frac{\Gamma(a+k)}{\Gamma(a)} = a(a+1)\cdot\cdots\cdot(a+k-1). \qquad \text{(A.3)}$$

Now, using the principle of Kummer (see [30] pp.42) we find:

$${}_1F_1\left(-\frac{1}{2},\frac{d}{2},-\frac{\lambda(t)}{2}\right) = \mathrm{e}^{-\lambda(t)/2}{}_1F_1\left(\frac{1+d}{2},\frac{d}{2},\frac{\lambda(t)}{2}\right) \qquad \text{(A.4)}$$

Therefore, by (A.3) and (A.4), Equation (A.1) reads:

$$\begin{aligned}
\mathbb{E}(\sqrt{v(t)}|v(0)) &= \sqrt{2c(t)}\mathrm{e}^{-\lambda(t)/2}\frac{\Gamma\left(\frac{1+d}{2}\right)}{\Gamma\left(\frac{d}{2}\right)}{}_1F_1\left(\frac{1+d}{2},\frac{d}{2},\frac{\lambda(t)}{2}\right) \\
&= \sqrt{2c(t)}\mathrm{e}^{-\lambda(t)/2}\frac{\Gamma\left(\frac{1+d}{2}\right)}{\Gamma\left(\frac{d}{2}\right)}\sum_{k=0}^{\infty}\frac{1}{k!}\left(\lambda(t)/2\right)^k\frac{\Gamma\left(\frac{1+d}{2}+k\right)}{\Gamma\left(\frac{1+d}{2}\right)}\frac{\Gamma\left(\frac{d}{2}\right)}{\Gamma\left(\frac{d}{2}+k\right)} \\
&= \sqrt{2c(t)}\mathrm{e}^{-\lambda(t)/2}\sum_{k=0}^{\infty}\frac{1}{k!}\left(\lambda(t)/2\right)^k\frac{\Gamma\left(\frac{1+d}{2}+k\right)}{\Gamma\left(\frac{d}{2}+k\right)},
\end{aligned}$$

which concludes the proof. □